

DISSERTATION

DEVELOPING A MODIFIED SEBAL ALGORITHM THAT IS RESPONSIVE  
TO ADVECTION BY USING LIMITED WEATHER DATA

Submitted by

Mcebisi Mkhwanazi

Department of Civil and Environmental Engineering

In partial fulfillment of the requirements

For the Degree of Doctor of Philosophy

Colorado State University

Fort Collins, Colorado

Summer 2014

Doctoral Committee:

Advisor: José Chávez

Allan Andales

Jay Ham

Thomas Trout

Copyright by Mcebisi Mkhwanazi 2014

All Rights Reserved

## ABSTRACT

### DEVELOPING A MODIFIED SEBAL ALGORITHM THAT IS RESPONSIVE TO ADVECTION BY USING LIMITED WEATHER DATA

The use of Remote Sensing ET algorithms in water management, especially for agricultural purposes is increasing, and there are more models being introduced. The Surface Energy Balance Algorithm for Land (SEBAL) and its variant, Mapping Evapotranspiration with Internalized Calibration (METRIC) are some of the models that are being widely used. While SEBAL has several advantages over other RS models, including that it does not require prior knowledge of soil, crop and other ground details, it has the downside of underestimating evapotranspiration (ET) on days when there is advection, which may be in most cases in arid and semi-arid areas. METRIC, however has been modified to be able to account for advection, but in doing so it requires hourly weather data. In most developing countries, while accurate estimates of ET are required, the weather data necessary to use METRIC may not be available.

This research therefore was meant to develop a modified version of SEBAL that would require minimal weather data that may be available in these areas, and still estimate ET accurately. The data that were used to develop this model were minimum and maximum temperatures, wind data, preferably the run of wind in the afternoon, and wet bulb temperature. These were used to quantify the advected energy that would increase ET in the field. This was a two-step process; the first was developing the model for standard conditions, which was described as a healthy cover of alfalfa, 40-60 cm tall and not short of water. Under standard conditions, when estimated ET using modified SEBAL was compared with lysimeter-measured

ET, the modified SEBAL model had a Mean Bias Error (MBE) of 2.2 % compared to -17.1 % from the original SEBAL. The Root Mean Square Error (RMSE) was lower for the modified SEBAL model at 10.9 % compared to 25.1 % for the original SEBAL.

The modified SEBAL model, developed on an alfalfa field in Rocky Ford, was then tested on other crops; beans and wheat. It was also tested on well-irrigated corn and also corn under deficit irrigation. The modified SEBAL model performed fairly well in wheat and beans, just slightly underestimating ET, and it performed well with irrigated corn. However, modified SEBAL, similar to the original SEBAL and also METRIC, could not accurately estimate ET for drier conditions or at early stages of plant growth.

## ACKNOWLEDGEMENTS

Firstly, I would like to express my sincere gratitude to my advisor and mentor Dr. José Chávez, who has guided me throughout my research. He has been very supportive, and I thank him for financially supporting me when my scholarship ended. I would also like to thank the rest of my PhD committee for their guidance, their encouraging messages, and comments meant to improve the quality of my work.

I also thank my colleagues, past and present, both in my Department and outside for their encouragement, and for being there when I needed them. In a special way, I thank Abhinaya Subedi, with whom I would discuss my research ideas; I wish him the best as he pursues his PhD.

Much thanks to the Institute of International Education (IIE)'s Fulbright Program, for awarding me the prestigious Science and Technology Scholarship. The Fulbright program has made this academic journey much easier than anticipated.

My gratitude also goes to my family; my parents and siblings, they have been wonderful. I can never be grateful enough; thank you for the love and support. A special thanks to my Mom, God knows Mvulane, the sacrifices you have made for me to be where I am today. Also much thanks to a special person, Noncedo, I have grown to depend on your love, support and mostly your patience, it has not been easy but you never gave up on us, I love you.

Last but most important, I thank God for all He's done for me. I do acknowledge that all that I have received is from Him.

## TABLE OF CONTENTS

### Contents

ABSTRACT.....	ii
ACKNOWLEDGEMENTS.....	iv
TABLE OF CONTENTS.....	v
CHAPTER 1 .....	1
Overview .....	1
INTRODUCTION.....	2
Remote Sensing Models .....	3
Description of SEBAL and METRIC Algorithms .....	5
Objectives .....	11
MATERIALS AND METHODS.....	11
Study Area.....	11
Landsat Satellite Datasets and Processing.....	12
Thermal Pixel Sharpening .....	13
Evaluation Criterion .....	14
RESULTS AND DISCUSSIONS .....	16
Hourly ET comparison .....	16
Daily alfalfa ET comparison.....	17
Possible causes of error in SEBAL daily ET estimation.....	19
Advection as cause for error in the estimation of daily ET with SEBAL .....	21
Model performance under varying wind and vegetation cover conditions .....	24
Effects of humidity on SEBAL model performance .....	25
CONCLUSIONS.....	28
RECOMMENDATIONS .....	29
REFERENCES .....	40
CHAPTER 2 .....	45
Overview .....	45
INTRODUCTION.....	46
EF constancy throughout the day .....	47
Objectives .....	49
MATERIALS AND METHODS .....	49
Study Area.....	49
Landsat Satellite Datasets and Processing.....	50
Description of procedure .....	51
Steps involved in the development of the advection sub-model .....	52
Requirement of wind data in SEBAL.....	57

RESULTS AND DISCUSSIONS .....	60
Parameterization of advection under standard conditions .....	60
Modified SEBAL testing .....	61
CONCLUSION .....	63
RECOMMENDATIONS .....	64
REFERENCES .....	71
CHAPTER 3 .....	75
Overview .....	75
INTRODUCTION.....	76
Surface roughness.....	77
Surface moisture availability .....	79
Description of BREB method.....	81
The BREB and advection .....	83
Objectives .....	84
METHODS AND MATERIALS .....	84
Study Area .....	84
Satellite Data Requirements and image processing.....	86
RESULTS AND DISCUSSIONS .....	87
CONCLUSION .....	91
RECOMMENDATIONS .....	92
REFERENCES .....	96
Overview .....	99
On the performance of SEBAL and METRIC: .....	101
Modification of SEBAL to account for advection: .....	102
Transferability of model to various surface conditions:.....	102
Summary of modification.....	103
Model Limitation (s).....	104
APPENDICES .....	105

# CHAPTER 1

## **Evaluating the performance of SEBAL and METRIC under advective and non-advective conditions**

### **Overview**

The use of remote sensing (RS) models in crop evapotranspiration (ET) estimation is aimed at improving agricultural water management. An example of a RS model that has been developed for this purpose is the Surface Energy Balance Algorithm for Land (SEBAL). One advantage that SEBAL has, is its minimal requirement for ground-based weather data. However, its downside is that in the presence of advection it may underestimate ET. This is mostly due to the use of a fixed evaporative fraction (EF) for the entire day. The EF value is used to extrapolate instantaneous ET to daily ET values, based on the assumption that EF determined at the time of satellite overpass remains constant throughout the day, and can therefore be used to estimate daily ET. The Mapping Evapotranspiration with Internalized Calibration (METRIC) model on the other hand, uses the alfalfa reference ET fraction ( $ET_r/F$ ), which is a ratio of actual crop ET to alfalfa reference ET, which enables the model to capture effects of advection. However, the use of  $ET_r/F$  requires good quality hourly weather data, which may be unavailable in some places (e.g. in developing countries), where only daily averages of weather data may be available. A study was carried out to compare these two models under varying conditions; varying weather conditions and under a range of vegetation cover conditions. A total of 27 Landsat 5 TM and Landsat 7 ETM+ images (2010-2012) were processed using both SEBAL and METRIC, and ET was estimated for two alfalfa fields near Rocky Ford in southeastern Colorado. Both fields were equipped with precision monolithic weighing lysimeters. The remotely sensed hourly and daily

ET values were compared with lysimeter-based ET measurements. Results showed that METRIC was more accurate than SEBAL in the estimation of ET. It was also observed that there were larger errors with SEBAL when there was advection (advection was indicated by higher wind speed, and warm and dry air). The results of this study indicate that, under conditions of advection, the use of SEBAL is not suitable, and that SEBAL should be modified to account for advection, and this could be achieved by using the daily averages of weather data.

## **INTRODUCTION**

Irrigation is one of the major consumptive users of water resources globally. Recently there has been an increasing competition for water use for urban, industry, tourism/entertainment, fracking and agricultural purposes. The phenomenon of a changing climate is also exacerbating an already serious situation. Studies published in research literature show how agricultural production especially in arid and semi-arid regions will be one of the sectors most vulnerable to climate change and variability (Challinor et al., 2005). The above-mentioned challenges make it necessary to improve agricultural water management (AWM). Improving AWM would involve accurate estimation of crop evapotranspiration (ET). ET is an essential component of the water balance or water cycle and it is a significant consumptive use of precipitation and water applied through irrigation on cropland (Paul et al., 2011).

Several methods have been used to directly or indirectly measure ET, and these include lysimeters, using reference ET and crop coefficients, eddy covariance method, the Bowen ratio surface energy balance method, scintillometry, atmometers, soil moisture sensors, and lately applying remote sensing (RS) techniques to estimate ET. The latter has an advantage of having a much larger or regional coverage unlike most methods, which have limited spatial coverage, or

even worse point measurements. Several RS methods have been developed. This study focuses on two of the methods; the Surface Energy Balance Algorithm for Land (SEBAL; Bastiaanssen et al., 1998) and Mapping Evapotranspiration with Internalized Calibration (METRIC; Allen et al., 2007), the latter making improvements on SEBAL. The study evaluates the performance of these two methods under advective and non-advective conditions in Rocky Ford, southeastern Colorado.

### **Remote Sensing Models**

Several RS models have been developed; SEBAL, METRIC, Remote Sensing of Evapotranspiration (ReSET; Elhaddad and Garcia, 2008), Analytical Land Atmosphere Radiometer Model (ALARM; Suleiman et al., 2009), Surface Aerodynamic Temperature (SAT; Chávez et al., 2010) and many other methods. SEBAL is capable of estimating ET without prior knowledge of the soil, crop, and management conditions (Bastiaanssen et al., 2005). METRIC is a modification of SEBAL and is based on the same principles, and both make use of the near surface temperature gradients ( $dT$ ) function as proposed by Bastiaanssen (Singh et al., 2008). SAT models aerodynamic surface temperature ( $T_o$ ), a variable that is not measured and not easily estimated. The surface temperature,  $T_o$  is used to determine sensible heat flux ( $H$ ), a component of the energy balance equation.

In the computation of  $H$ , other methods often use radiometric surface temperature ( $T_s$ ) instead of  $T_o$ , and this may result in the overestimation of  $H$  and thus underestimation of crop ET (Chávez et al., 2010). The ReSET model, unlike the original versions of SEBAL and METRIC does not assume that the weather parameters from one weather station could be applicable for the whole area represented in an image which is very large (e.g. 185 x 172 km for Landsat 5

images). However, ReSET takes into consideration the spatial variability of weather parameters. ReSET interpolates for weather data between available weather stations in time and space (Elhaddad and Garcia, 2008).

Gowda et al. (2008) classified RS methods by their approach in the estimation of ET; the first category being those methods that employ the land surface energy balance (EB) and the second are those that use a reflectance based crop coefficient approach. The RS EB-based methods can also be classified as one-source or two-source models. In a one-source model, a heterogeneous surface is represented as a single layer (Chávez et al., 2009) and the energy balance components are determined as coming from one source.

The two-source approach models the energy balance of soil and vegetation separately (Gowda et al., 2008). Hipps and Kustas (2000) mentioned that there is a problem when a heterogeneous surface is represented as a single source as soil has a significant influence on the surface energy balance. However, the two-source model requires several assumptions, for example in the partitioning of radiometric surface temperature into that of soil and of vegetation, also in coupling/decoupling energy exchange between soil and vegetation (Chávez et al., 2009). Even though theoretically the two-source method is expected to perform better, Li and Lyons (1999) evaluated RS based models for ET and found that the single-source performed better than the two-source models, probably due to the number of assumptions associated with the latter.

This chapter discusses SEBAL and its variant METRIC. One reason for focusing on SEBAL is that it has been widely applied for ET estimation in different countries under different agro-climatic conditions (Singh et al., 2008). Allen et al. (2005) outlines few advantages that SEBAL and METRIC have over other RS methods in estimating ET. Some of the advantages being that the methods do not require knowledge of crop type; they both have some internal

calibration of sensible heat flux computation, which according to the authors eliminates the need for atmospheric correction. Singh et al. (2008) also mention that the use of a  $dT$  function in  $H$  estimation prevents the error that can be incurred due to the use of surface radiometric temperature instead of surface aerodynamic temperature. This concept is discussed later under model description.

SEBAL has however the limitation of not being able to account for advection (Singh et al., 2008; Allen et al., 2005), hence the introduction of METRIC which has the capability to incorporate effects of advection. However METRIC requires good quality hourly data of solar radiation, air temperature, and relative humidity and wind speed. Such data may not be available in some parts of the world especially in developing countries. Therefore, where advection is not a factor, SEBAL has the advantage of requiring minimal weather data. However, for places where there is advection, and there is not enough data to employ METRIC, a new model needs to be developed, which would require less weather data, such as daily averages, while at the same time adequately accounting for advection.

### **Description of SEBAL and METRIC Algorithms**

Images obtained from the satellite (e.g. Landsat TM 5 & ETM+ 7) are in raster formats, with pixels of 30 m by 30 m for the visible bands and infrared, and these are processed using RS models and GIS software (e.g. ArcGIS, ERDAS Imagine.). SEBAL and METRIC both estimate ET through the land surface energy balance (EB) method, using remotely sensed surface reflectance in the visible and near infrared portions of the electromagnetic spectrum. The radiometric surface temperature is measured using the satellite thermal infrared band. The approach is to convert the satellite-sensed radiances into land surface characteristics that include

surface albedo, leaf area index, vegetation indices, surface emissivity, and surface temperature. These variables are then used to calculate the various components of the energy balance; net radiation ( $R_n$ ), soil heat flux ( $G$ ) and the sensible heat flux ( $H$ ), then the latent heat flux ( $LE$ ) is obtained as a residual, as given in Equation 1.1.

$$LE = R_n - G - H \quad (1.1)$$

**Net Radiation** - SEBAL and METRIC do not differ much in the estimation of  $R_n$  and  $G$ . The net radiation is calculated by summing the net shortwave radiation and net longwave radiation. In SEBAL, the net radiation is determined as shown in Equation 1.2:

$$R_n = (1 - \alpha)R_s + \varepsilon_a \sigma T_a^4 - \varepsilon_s \sigma T_s^4 \quad (1.2)$$

where  $R_s$  is incoming shortwave radiation ( $\text{W m}^{-2}$ ),  $\alpha$  is the surface albedo which is the ratio of reflected to solar radiation incident at the surface,  $\varepsilon_a$  is the air thermal emissivity,  $\varepsilon_s$  is surface thermal emissivity,  $T_a$  is the air temperature,  $T_s$  is the radiometric surface temperature (K), and  $\sigma$  is the Stefan Boltzmann constant which is equal to  $5.67 \times 10^{-8} \text{ W m}^{-2} \text{ K}^{-4}$ .

METRIC has an additional component, giving  $R_n$  as shown in Equation 1.3:

$$R_n = (1 - \alpha)R_s + \varepsilon_a \sigma T_a^4 - \varepsilon_s \sigma T_s^4 - (1 - \varepsilon_s)\varepsilon_a \sigma T_a^4 \quad (1.3)$$

The added component in METRIC takes into account that there is surface reflectance of the incoming longwave radiation.

**Soil heat flux** - it is defined as the rate of heat flow into the soil due to conduction (Gowda et al., 2011). Different empirical equations have been developed, based on extensive soil heat flux measurements made in experimental fields (e.g. Singh et al., 2008; Bastiaanssen et al., 1998). The one used in this study (Equation 1.4) was developed by Bastiaanssen (1995).

$$\frac{G}{R_n} = \frac{T_s}{\alpha} (0.0038\alpha + 0.0074\alpha^2)(1 - 0.98NDVI^4) \quad (1.4)$$

where  $\alpha$  and  $T_s$  are as defined in Equation 1.2. The NDVI is the Normalized Difference Vegetation Index, which is computed using surface reflectance captured using bands 3 and 4 in Landsat 5 and 7. Band 3 is the visible red and 4 is the near infrared, with wavelengths approximately 0.6-0.69  $\mu\text{m}$  for red and 0.75-0.9  $\mu\text{m}$  for near infrared. The exact values depend on the particular satellite's instruments.

**Sensible heat flux** - the basic calculation of H is performed by using the bulk aerodynamic resistance method as shown in Equation 1.5:

$$H = \frac{\rho_a c_{pa} (T_o - T_a)}{r_{ah}} \quad (1.5)$$

where  $\rho_a$  is the density of moist air ( $\text{kg m}^{-3}$ ),  $C_{pa}$  is specific heat capacity of dry air ( $\sim 1004 \text{ J kg}^{-1} \text{ K}^{-1}$ );  $T_a$  is the average air temperature (K) at screen height (typically at 2 m),  $T_o$  is the average surface aerodynamic temperature (K), and  $r_{ah}$  is the aerodynamic resistance to heat transfer ( $\text{s m}^{-1}$ ). However,  $T_o$  may be difficult to estimate, therefore SEBAL and METRIC replace  $(T_o - T_a)$  by a dT function as shown in Equation 1.6, and the dT function is defined as the near surface temperature difference between two levels, which are 2 m and 0.1 m (Allen et al., 2011).

$$H = \frac{\rho_a c_{pa} dT}{r_{ah}} \quad (1.6)$$

In the process of determining the dT function, two extreme pixels, a wet and dry pixels, are selected. In the selection of a wet pixel, it is a pixel that has a low temperature; with the assumption that the low temperature is so because the available energy ( $R_n - G$ ) is mostly used to evaporate water and not to warm the surface. Originally in SEBAL, a water body was selected for the wet or cold pixel (Allen et al., 2011). However, it is now recommended that a pixel

located in a well-watered agricultural field of good crop growth be selected. In SEBAL it is assumed that all the available energy is used for evaporation, therefore at the wet/cold pixel  $H$ , is assumed to be zero. The LE in that pixel therefore equals the available energy. This is a reasonable assumption, except in semi-arid and arid regions, where there could be regional horizontal advection of sensible heat energy brought into the irrigated area and used for evaporation enhancement, in which case  $H$  would be negative, and not zero.

According to Equation 1.6, the value of  $dT$  in the cold pixel will be zero following the assumption that  $H$  equals zero. For METRIC, in the selection of a wet pixel, an agricultural field of good crop growth is used. However instead of assuming a zero value for  $dT_{cold}$  for that pixel,  $dT_{cold}$  is given as:

$$dT_{cold} = \frac{(R_n - G - 1.05\lambda ET_r)r_{ah}}{\rho_a C_p} \quad (1.7)$$

where,  $R_n$  and  $G$  are satellite-determined, and are specifically for that cold pixel,  $ET_r$  is the hourly alfalfa reference ET ( $\text{mm h}^{-1}$ ) computed for an alfalfa reference using weather data from the area of study, and  $\lambda$  is the latent heat of vaporization ( $\text{J kg}^{-1}$ ) which is used to convert  $ET_r$  ( $\text{mm h}^{-1}$ ) to latent heat flux ( $\text{W m}^{-2}$ ), and is obtained as shown in Equation 1.8.

$$\lambda = (2.501 - 0.00236T_s) \times 10^6 \quad (1.8)$$

In Equation 1.7,  $ET_r$  is multiplied by 1.05 assuming that a pixel selected would be an area with large vegetation biomass and will have a larger surface wetness and therefore should have ET that is about 5% greater than  $ET_r$  (Allen et al., 2005). The use of  $ET_r$  in METRIC makes it responsive to advective conditions, as LE can be larger than  $(R_n - G)$ , thus giving a negative  $H$  value on well-irrigated fields when there is advection.

To select a dry pixel, a hot pixel with a high temperature would be a candidate since it would indicate extreme dryness since the solar energy incident on the surface is used to heat up the surface and air above it instead of evaporating water. In addition, the pixel should either be bare or have minimal biomass, which is indicated by a low leaf area index value. Care should be taken that man-made surfaces such as highways and buildings are not selected. A dry agricultural area (possibly fallow) or bare soil is recommended. This pixel is assumed to have LE of zero, and a large dT.

While both models would initially assume LE of zero in the dry pixel, in METRIC if there has been a wetting event recently, a daily surface soil water balance is run for the hot pixel using the two-stage evaporation process as described by Allen et al. (1998) in order to confirm that LE equals zero or to supply a nonzero value instead. Once the dry/hot pixel is identified, the value of H can be calculated using the  $R_n$  and G from the image for that pixel. The dT value can then be calculated using Equation 1.9:

$$dT_{hot} = \frac{(R_n - G)r_{ah\ hot}}{\rho_{air\ hot}c_p} \quad (1.9)$$

Both models then assume a linear relation of dT to radiometric surface temperature and the relationship is explained by the use of coefficients 'a' and 'b' whereby:

$$dT = a \times T_s + b \quad (1.10)$$

where:

$$a = \frac{dT_{hot} - dT_{cold}}{T_{s\ hot} - T_{s\ cold}} \quad b = dT_{hot} - a \times T_{s\ hot}$$

To obtain the value of H, Equation 1.6 is used and this value is corrected for atmospheric stability, which involves an iterative process using the Monin-Obhukov similarity theory.

SEBAL and METRIC differ in the extrapolation of instantaneous ET to daily ET values. SEBAL uses evaporative fraction (EF), which is defined as the ratio of LE to available energy ( $R_n - G$ ). EF is calculated for each pixel, for the time of the remote sensing platform overpass, as:

$$EF = \frac{LE}{R_n - G} \quad (1.11)$$

All the fluxes are instantaneous. In SEBAL, this fraction is assumed to remain constant throughout the day, and can therefore be used in the extrapolation of LE obtained for short periods to hourly and daily values, therefore giving daily ET ( $ET_{24}$ ) as:

$$ET_{24} = \frac{86,400 \times EF \times (R_{n24} - G_{24})}{\lambda \times \rho_w} \quad (1.12)$$

where 86,400 is the number of seconds in a day, and  $R_{n24}$  is the average net radiation ( $W\ m^{-2}$ ) for the day;  $\lambda$  is the latent heat of vaporization used to convert the energy from  $W\ m^{-2}$  to mm of evaporation or vice-versa and is a function of temperature, and  $\rho_w$  is the density of water in  $kg\ m^{-3}$ .  $G_{24}$  is the daily average of soil heat flux ( $W\ m^{-2}$ ) and is negligible for vegetation and soil surfaces on a 24-h period, as it is assumed that the energy stored in the soil during the day is lost at night.

The assumption of a conserved EF has been widely accepted and generally used (Nichols and Cuenca, 1993; Crago and Brutsaert, 1996; Suleiman et al., 2009). However, Gentine et al. (2011) stated that EF is rarely constant, though more likely to be constant under conditions of higher relative humidity (75-90%). In semi-arid regions, the EF constancy may not apply. Lhomme and Elguero (1999) also stated that the assumption of a constant diurnal EF results in significant error in conditions of advection.

METRIC, instead of using EF, uses the fraction of alfalfa reference ET ( $ET_rF$ ). This is the ratio of the actual crop ET to  $ET_r$  at the time of overpass, and it is also assumed to be constant

throughout the day. The daily ET is therefore obtained by multiplying  $ET_{rF}$  by  $ET_{r-24}$  the latter being  $ET_r$  for the day, obtained by summing hourly reference ET for the entire day. This approach is capable of capturing most of the advection impacts and any other change in weather conditions during the day.

## **Objectives**

It has been mentioned that SEBAL is unable to account for advection, therefore resulting in underestimation of ET when there is advection. It is therefore the objective of this chapter to evaluate the performance of SEBAL and METRIC under advective and non-advective conditions, and assess how significant the error due to advection is. In addition, the effects of vegetation surface cover on the accuracy of the models were evaluated.

## **MATERIALS AND METHODS**

### **Study Area**

This research was carried out at Colorado State University (CSU) Arkansas Valley Research Center (AVRC) near Rocky Ford, in southeastern Colorado. Irrigated fields surrounded by dry areas in southeastern Colorado are shown in Figure 1.1. The study area has geographic coordinates  $38^{\circ} 02' N$ ,  $103^{\circ} 41' W$ , with an elevation of 1,274 m above mean sea level (amsl). The area receives an average annual precipitation of about 300 mm, with 65 % falling in May through September. The summer average temperature is  $23.6^{\circ} C$ , and the average daily maximum is  $33^{\circ} C$ . The average relative humidity in the mid-afternoon is 25 % in summer, and average wind speed is  $4.4 m s^{-1}$ .

Two fields were used for the study, both planted to alfalfa which was irrigated using a furrow irrigation system supplied by siphons and a head ditch. Field A was rectangular, 160 m by 250 m, and Field B was triangular (right-angled, with base 110 m and perpendicular length of 230 m). Close to the center of Field A was a large monolith weighing lysimeter (3 m × 3 m × 2.4 m deep), and a smaller lysimeter (1.5 m × 1.5 m × 2.4 m deep) was in Field B. Both fields were equipped with net radiometers (REBS, Campbell Scientific International (CSI), Logan, Utah, U.S.A.). There were also infrared thermometers (IRT, Apogee model S1-111, CSI, Logan, Utah, U.S.A.) to measure crop radiometric surface temperature. Soil heat flux plates (REBS model HFT3, CSI, Logan, Utah, U.S.A.) were buried in the ground at locations proximal to the measurements of net radiation at a depth of about 10 cm, along with soil temperature and soil water sensors, to aid in the estimation of stored soil heat, and subsequently soil heat flux at the surface.

### **Landsat Satellite Datasets and Processing**

Landsat 5 Thematic Mapper (TM) and Landsat 7 Enhanced Thematic Mapper Plus (ETM+) cloud free satellite images were downloaded from the USGS Earth Explorer site [<http://edcsns17.cr.usgs.gov/NewEarthExplorer/>] for the 2010-2012 growing seasons. In total, 23 images were downloaded and used for hourly ET analysis and 20 for daily ET analysis. The 3 images that were not used for daily ET analysis was because of activity taking place in the field on the day of satellite overpass (e.g. maintenance, harvesting or irrigation but not during the hour of overpass). The temporal resolution (or revisit period) is 16 days for both satellites, with alternating coverage. Therefore if cloud cover or the swaths of missing data for Landsat 7 do not affect images, the number of days between overpasses is 8. Both satellites provide images at a

spatial resolution of  $30 \times 30$  m in the visible and near infrared portions of the electromagnetic spectrum. The thermal infrared band for Landsat 5 has a spatial resolution of  $120 \text{ m} \times 120 \text{ m}$  while Landsat 7 has a spatial resolution of  $60 \text{ m} \times 60 \text{ m}$ .

### **Thermal Pixel Sharpening**

Due to the research fields being relatively small, a thermal resolution of  $120 \times 120$  m for Landsat 5 and  $60 \times 60$  m for Landsat 7 may result in contaminated pixels from adjacent fields and/or roads. To avoid this, thermal sharpening was carried out for each image, based on documented evidence that there is a relationship between percent ground cover and surface temperature (Badeck et al., 2004). Due to the fact that percent ground cover is highly correlated to NDVI, the latter was used as a surrogate for ground cover, as has been used in many sharpening approaches (Wonsook et al., 2010; Allen et al., 2008; Agam et al., 2008).

The process was carried out for each image because the relationship between ground cover and surface temperature is not constant but varies with weather and surface conditions and land cover type (Karnieli et al., 2006). The process involved selecting 25 pixels from fields large enough to have several uncontaminated pixels. These were selected from across the whole image or its subset. The pixels selected varied from partial to full cover. From each pixel selected, the NDVI, surface temperature and reflectance for bands 5 and 7 were noted. The 25 pixels were then randomly divided into training and testing (validating) datasets; 15 pixels for the training dataset, and 10 for the testing dataset. The training dataset was then used to establish the relationship between the NDVI and the radiometric surface temperature. The equation relating the NDVI to radiometric surface temperature from the training dataset was then used to estimate surface temperature, using NDVI from the testing dataset, and the estimated temperature was

compared with the observed temperature. The deciding factor on the appropriateness of the regression was the  $RMSE/\sigma$ , where  $\sigma$  is the standard deviation of  $T_s$  from the testing dataset and RMSE is the Root Mean Square Error, a statistic that is explained later. According to Kustas and Norman (2000), a value of approximately 1 indicates poor agreement between estimations and observations, while  $< 0.5$  means the approach is capable of estimating values and is in satisfactory agreement with observations. In this study, if  $RMSE/\sigma$  was less than 0.5, then the relationship was used for the whole scene to process a new image for surface temperature at a refined resolution of  $30\text{ m} \times 30\text{ m}$ .

Table 1.1 shows the equations developed and thereafter used in the adjustment of surface temperature. It must be noted that the thermal pixel sharpening method may incur some errors for wet/moist bare soil, which may have lower temperatures due to moist conditions; such surfaces will have a low NDVI and lower temperatures, thus not following the pattern. This can however be detected by using bands 5 or/and 7 as they can identify bare soils that are moist, and these are then excluded from the datasets.

## **Evaluation Criterion**

Comparison was made between the alfalfa ET estimated using the remote sensing algorithms with the alfalfa ET measured using the lysimeters. The comparison was for hourly and daily time-steps. Several indicators were used to measure the model performance in estimating ET, and they are defined as follows:

**Coefficient of determination ( $R^2$ ):** This is a measure of the proportion of variance in measured data that is explained by a model. It allows one to determine the certainty of making a prediction

from a model. It ranges between 0 and 1, with a value of 1 being the optimal. Typically, a value that is greater than 0.5 is considered acceptable.

$$R^2 = \frac{(\sum_i^n (O_i - \bar{O})(M_i - \bar{M}))^2}{\sum_i^n (O_i - \bar{O})^2 \times \sum_i^n (M_i - \bar{M})^2} \quad (1.13)$$

where O is the observed (measured) value and M is the predicted or derived (remote sensing based in this case) value. The bars above the variables denote averages.

**Mean Bias Error (MBE):** This indicator is usually used to determine the average model bias or average over- or under-prediction. MBE is obtained by summing up the differences between predicted and observed values, then dividing by the number of compared pairs. Positive values indicate model over-estimation bias, and negative values indicate model under-estimation bias (Willmott 1982; Katiyar et al., 2010), and zero is interpreted as absence of bias and not necessarily absence of error.

$$MBE = \frac{1}{n} \sum_i^n (M_i - O_i) \quad (1.14)$$

**Root Mean Square Error (RMSE):** This is a commonly used error index statistic. A smaller RMSE value indicates a smaller error spread and variance and therefore a better model performance. It measures the magnitude of the spread of errors, squaring errors before averaging them. Therefore, the RMSE gives a relatively high weight to large errors. Willmott (1982) defines RMSE as:

$$RMSE = \sqrt{\frac{1}{n} \sum_i^n (M_i - O_i)^2} \quad (1.15)$$

**Nash-Sutcliffe Coefficient of Efficiency (NSCE):** This is usually used to assess the predictive ability of a model. To determine NSCE, the sum of squared differences between the predicted

and observed values, normalized by the variance of the observed values is subtracted from one. NSCE values range between  $-\infty$  and 1. The closer the model efficiency is to 1, the more accurate the model is, with values above zero indicating an acceptable performance level, while values less than zero indicate unacceptable performance (Moriassi et al., 2007; Nash and Sutcliffe, 1970).

$$NSCE = \frac{\sum_i^n (O_i - \bar{O})^2 - \sum_i^n (M_i - O_i)^2}{\sum_i^n (O_i - \bar{O})^2} \quad (1.16)$$

where “M” is the model estimation or prediction for ET, either for SEBAL or METRIC models, “O” is the measured or observed ET, and “n” is the number of observations.

## RESULTS AND DISCUSSIONS

### Hourly ET comparison

The hourly alfalfa ET estimated using SEBAL and METRIC were compared with those measured using the large monolithic weighing lysimeter. There was observed an MBE of  $-0.09 \text{ mm h}^{-1}$  (-12%) for SEBAL and  $-0.11 \text{ mm h}^{-1}$  (-15%) for METRIC, so both methods on average slightly underestimated ET. Figures 1.2 and 1.3 show how SEBAL and METRIC ET compared with lysimeter ET, with METRIC having more points below the 1:1 line (underestimation), though most of them were closer to the line than in the case of SEBAL ET. For the other indicators (i.e. RMSE,  $R^2$  and NSCE), METRIC seemed to perform better than SEBAL, but the differences were not large. The NSCE values for both models were within the acceptable range of model performance; 0.5 for SEBAL and 0.67 for METRIC.

The hourly ET comparison for each day is given in detail in Table A1 in Appendices; and from the results, SEBAL had a maximum estimation error of 39% while METRIC had a maximum error of 27%. This analysis excluded the dates with asterisks (02 August 2010 to

05 October 2010) in Field B, where the field was bare and therefore had very low vegetation cover; in which case the model gave errors of up to 100%.

### **Daily alfalfa ET comparison**

Figures 1.4 and 1.5 show daily ET for SEBAL and METRIC, respectively. While both methods tend to underestimate ET when compared to the lysimeter, there is greater extent of underestimation with SEBAL, with MBE of  $-2.6 \text{ mm d}^{-1}$  (-32%) and  $-1.7 \text{ mm d}^{-1}$  (-20%) for METRIC. RMSE was  $3.18 \text{ mm d}^{-1}$  and  $1.99 \text{ mm d}^{-1}$  for SEBAL and METRIC, respectively. The NSCE for SEBAL was -0.07 which indicates an unacceptable performance of the model in estimating alfalfa daily ET. METRIC had an acceptable NSCE value of 0.58. Therefore, while the SEBAL model was appropriate in estimating hourly ET (NSCE = 0.5), in the estimation of daily ET the model was found to be unsuitable (NSCE = -0.07).

The reason SEBAL would be suitable to estimate ET on hourly basis and not suitable on daily basis could be due to the use of EF in extrapolating instantaneous ET to daily values. The extrapolation assumes that the EF at the time of satellite overpass remains constant throughout the day, which is sometimes not the case with occurrence of afternoon advection as might have been the case in this study. The table in Appendix A2 shows the error for daily ET estimation as high as 48 % for SEBAL, which is higher when compared to what others have previously observed. Gowda et al. (2008) reported an average accuracy of 85 % (i.e., 15 % error) for a single day, while Trezza (2002) found the error to range from 2.7 to 35 %, 18.2 % being the average error. Singh et al. (2008) found that estimated  $ET_c$  using SEBAL was within 5 % of measured  $ET_c$ . However, he also observed that on certain advective days, SEBAL underestimated ET, as in one day he observed estimated  $ET_c$  being 28 % lower than measured

ET<sub>c</sub>. Allen et al. (2005) found that differences between METRIC-estimated and lysimeter-measured ET were less than 4 % over an entire crop growth season. He also pointed out that errors as high as 10-20 % are tolerable if they are random.

For both SEBAL and METRIC, and at both time-steps, i.e. hourly and daily, there was more discrepancy between estimated and measured ET when the fields had low vegetation cover. This could be because the models may be inappropriate to estimate ET from less vegetated surfaces. Hips and Kustas (2000) explained the complications that are brought about by surface heterogeneity in the estimation of ET. Heterogeneity at the canopy level is when the source of latent heat differs from that of sensible heat (Shuttleworth and Wallace, 1985 as cited by Hips and Kustas, 2000). Therefore patchy surfaces with low biomass may be considered heterogeneous. Hips and Kustas (2000) further explained that with homogenous surfaces, the ratio of roughness length of momentum ( $Z_{om}$ ) to that of heat ( $Z_{oh}$ ) is constant, but then varies for surfaces with partial canopy. The uncertainties surrounding the change in the ratio may cause errors in the determination of H and LE.

Also with less cover, the H and G components of the energy balance are large and therefore play a significant role, and these in most cases incur more error in their estimation than  $R_n$ , which is mostly accurately estimated. The estimation of H may be prone to error as it involves some subjective selection of extreme pixels. Therefore if the whole process of H estimation is not accurately done, as it depends on availability of appropriate extreme pixels and also experience, the error on ET may be significant. Also, the estimation of G may require locally developed empirical equations, and several equations have been developed based on local measurements of soil heat measurements (Singh et al., 2008; Chavez et al., 2005). However with

full cover or well-irrigated fields, both the H and G components are small and any error in their estimation will have less impact on the final LE or ET map.

### **Possible causes of error in SEBAL daily ET estimation**

As earlier explained, SEBAL and METRIC make use of the energy balance equation (Equation 1.1), and these estimate  $R_n$ , H and G, and then obtain LE as a residual. The estimation of these components of the energy balance should therefore be as accurate as possible. In both SEBAL and METRIC,  $R_n$  is determined using satellite-detected broadband surface reflectance and radiometric temperature (Allen et al., 2005), and G is related to  $R_n$ . The estimation of G becomes of less importance in vegetated and well-watered surfaces, as G is small under those conditions. Both SEBAL and METRIC usually estimate  $R_n$  well, within 5 % error. They also both have built-in mechanisms to compensate for bias that might have occurred in  $R_n$  and G estimation. By fixing the H and LE in the extreme pixels in the H sub-model, the bias is reduced. Therefore, as long as there are appropriate extreme pixels in the scene and the selection process of these pixels is done correctly, there will be less error that will be contributed by instantaneous  $R_n$  and G, in a well-vegetated surface, in the overall estimation of LE.

In SEBAL, the estimation of daily ET is as illustrated in Equation 1.12,  $G_{24}$  is assumed to be zero as earlier explained. The day average of net radiation ( $R_{n24}$ ) is determined either from measured incoming solar radiation ( $R_s$ ) using instruments (e.g., pyranometer) or determined by using a calculated extraterrestrial solar radiation ( $R_a$ ). On a cloudless day, about 75 % of extraterrestrial radiation is estimated to reach the earth's surface, and less on cloudy days. This is an estimate, and the value depends on atmospheric conditions. As radiation penetrates the

atmosphere, some of it is absorbed, some scattered, and some reflected by atmospheric gases, water vapor and solid particles. In SEBAL,  $Rn_{24}$  is then obtained as shown in Equation 1.17.

$$Rn_{24} = (1-\alpha)Ra_{24}\tau_{sw} - 110\tau_{sw} \quad (1.17)$$

where  $Ra_{24}$  is the daily extra-terrestrial radiation and  $\tau_{sw}$  is the one-way short-wave radiation transmittance. This equation is appropriate for cloud-free days, otherwise if there have been clouds during the course of the day, the  $Rn_{24}$  may be overestimated resulting in overestimation of ET. On such days, it is recommended to measure solar radiation on site or obtain readings from neighboring weather stations to obtain an accurate value of solar radiation for that particular day. In developing countries, where the costly equipment used to measure solar radiation may not be available on site and there may be none in neighboring stations, sunshine cards could be used to determine the relative sunshine duration ( $n/N$ ), which is a ratio that expresses the cloudiness of the atmosphere (Allen et al., 1998). Relative sunshine duration is defined as the ratio of actual duration of sunshine ( $n$ ) to the maximum possible duration of sunshine or daylight hours ( $N$ ).

To evaluate the accuracy of Equation 1.17 in estimating  $Rn_{24}$ , the estimated  $Rn_{24}$  was compared with  $Rn_{24}$  measured using a net radiometer (REBS, Campbell Scientific International (CSI), Logan, Utah, U.S.A.). The comparison was carried out on Area A, on selected days in 2010 when the alfalfa was at full cover. A total of 19 days were used, on days with clouds and also on cloud-free days. Table A3 in Appendices shows the comparison of calculated and measured  $Rn_{24}$ , with calculated  $Rn_{24}$  slightly higher than measured  $Rn_{24}$  (by  $10 \text{ W m}^{-2}$  on average; which is an ET equivalent of  $0.35 \text{ mm d}^{-1}$ ). When only cloud-free days were considered, the overestimation was a mere  $0.3 \text{ W m}^{-2}$ ; which is an ET equivalent of  $0.01 \text{ mm d}^{-1}$ . On the cloudiest day observed in the comparison,  $Rn_{24}$  was overestimated by  $66 \text{ W m}^{-2}$ ; which is  $2.3 \text{ mm d}^{-1}$  as ET. Figures 1.6 and 1.7 show the pattern of  $R_n$  over the course of the day, with Figure

1.6 showing a smooth curve on a cloud free day, and Figure 1.7 showing a rugged graph on a cloudy day.

In this study, it can be concluded that  $Rn_{24}$  estimation could not be the cause of the underestimation of the SEBAL model of ET as Table A3 in Appendices has shown that there is minimal error on cloud-free days, and on cloudy days the measured solar radiation was used to determine  $Rn_{24}$ . Even if the calculated  $Rn_{24}$  were to be used for cloudy days, it would cause overestimation and not the underestimation as given by the SEBAL model.

### **Advection as cause for error in the estimation of daily ET with SEBAL**

The  $Rn_{24}$ , either calculated or measured is however not the only source of energy that is used as latent heat, but extra energy is sometimes brought to the evaporating surface as advection. The energy available for daily ET consists of  $Rn_{24}$  and some advected energy, which SEBAL does not account for, as evidenced in Equation 1.12. It could therefore be hypothesized that the discrepancy observed between the SEBAL-modeled ET and the lysimeter-measured ET could be the result of not incorporating advected energy in Equation 1.12.

An attempt to test that hypothesis was made by relating advected heat flux to the observed daily errors. The definition of advection used in this study was that of Zermono-Gonzalez and Hipps (1997), where they define advection as “the horizontal transport of heat and humidity resulting from surface inhomogeneity”. They point out that effects of advection are more pronounced in arid and semi-arid regions, where irrigated fields are surrounded by dry lands.

Using the lysimeter ET results, and measured  $R_n$ ,  $G$  and  $T_s$ , using instruments in the field, an energy balance equation was used to obtain  $H$ . All the fluxes, i.e.  $LE$ ,  $R_n$  and  $G$  were

calculated or measured as averages at 15 minutes intervals and were then reported as daily averages. In most cases, LE exceeded the “vertical” available energy ( $R_n - G$ ), therefore giving a negative H. This is a reasonable occurrence since the days selected for this part of the study were days when the alfalfa was not short of water, with the instantaneous EF being at least 0.95.

It is worth noting that the experimental fields are in the vicinity of irrigated area that is surrounded by a vast dry area. Figure 1.8 suggests that the errors, which are the discrepancies between SEBAL-modeled and lysimeter-measured ET, are strongly correlated to the negative H values obtained using the energy balance equation based on data collected at the lysimeter ( $R^2 = 0.96$ ), which suggest that the underestimations were largely due to advection.

To further support the influence of advection on the SEBAL underestimation of daily ET, the relationship between the daily average evaporative fraction ( $EF_{24}$ ) and % error incurred with SEBAL in the estimation of ET was developed. This was achieved by first calculating the daily average latent heat flux ( $LE_{24}$ ) by using the lysimeter measured ET. The daily average net radiation ( $Rn_{24}$ ) and daily average soil heat flux ( $G_{24}$ ) were obtained from the net radiometer and soil heat flux plates (installed at the lysimeter), respectively. These daily averages were calculated from measurements of the various fluxes taken from the field every 15 minutes.  $EF_{24}$  was then calculated as follows:

$$EF_{24} = \frac{LE_{24}}{Rn_{24} - G_{24}} \quad (1.18)$$

A relationship was then drawn between  $EF_{24}$  and SEBAL % ET error for conditions of alfalfa with no water stress and with standard crop height canopy of 40-60 cm. The conditions of non-stress were identified by selecting pixels with instantaneous EF ( $EF_{inst.}$ ) with a value of at least 0.95. Figure 1.9 shows the result of fitting a polynomial curve relating  $EF_{24}$  to % error in daily ET estimation, with the error increasing with increasing EF. EF of more than 1 suggests

advective conditions as the latent heat exceeds the available energy; which means the excess energy would be coming from outside the area of interest.

De Bruin et al. (2005) mentioned that high wind speed, high air temperature and low humidity levels signal the occurrence of advection. In their paper, they termed these parameters advection indicators. Brakke et al. (1978) also made a similar observation that regional advection depends on wind speed. In this study, a relationship was drawn between wind speed and the error incurred by the SEBAL model on estimating daily alfalfa ET as shown in Figures 1.10, 1.11 and 1.12. Figure 1.10 used average wind speed over a 24-hr day, while Figure 1.11 used average wind speed over the daytime (when  $R_n > 0$ ), when most of the ET occurs, and then Figure 1.12 used the afternoon average wind speed (between noon and when  $R_n$  decreases to 0), when the air is warmer and drier, hence more advected energy. There seemed to be a stronger correlation with the latter, suggesting that the errors in the SEBAL model were mostly due to the afternoon advection, which the SEBAL model could not account for.

The shape of the curves is also worth noting, especially with Figures 1.11 and 1.12, where at low wind speeds ( $<1.5 \text{ m s}^{-1}$ ), the errors seem to be independent of the wind speed, but for winds greater than  $1.5 \text{ m s}^{-1}$  there was an obvious relationship between wind speed and model error, in this case being model underestimation, with the error increasing with increasing wind speed until around  $4 \text{ m s}^{-1}$  when increasing wind speed did not result in increased error. The presence of error for wind speed less than  $1.5 \text{ m s}^{-1}$  may have been a result of local rather than regional advection. Usually local advection is a small proportion of the total advection in cases where both forms occur, about a fifth of the total advection effect on ET, and the local advection is usually unrelated to wind speed (Brakke et al., 1978). It may be for that reason therefore, that at low wind speeds with drier and warm air, there could still be some error when using SEBAL.

The leveling off at about  $4 \text{ m s}^{-1}$  could be due to the fact that the higher wind speed may result in a higher evaporative demand which the alfalfa cannot meet, and therefore resulting in a response by the alfalfa in the form of reduced stomatal conductance. Zermeno-Gonzalez and Hipps (1997) observed an inverse relationship between canopy moisture conductance and saturation deficit at the canopy surface. This may explain the plateau of SEBAL ET error at high wind speeds.

### **Model performance under varying wind and vegetation cover conditions**

Tables 1.2 and 1.3 show the performance of the models (i.e., SEBAL and METRIC) for different wind speeds and also different vegetation fractions as indicated by leaf area index (LAI). In Table 1.2, the indicators show that SEBAL can better estimate ET under low wind conditions ( $0 - 2 \text{ m s}^{-1}$ ) than windy conditions ( $> 2 \text{ m s}^{-1}$ ). More windy conditions may be indicative of conditions of advection in this region. This is a similar observation to previous ones, i.e. under advective conditions the model underestimates daily alfalfa ET. In this case, when the wind speed was less than  $2 \text{ m s}^{-1}$ , the MBE was about  $-1.4 \text{ mm d}^{-1}$  (-17 %), whereas with wind speed above  $2 \text{ m s}^{-1}$  the MBE increased to  $-3.8 \text{ mm d}^{-1}$  (-40 %). This is when 24-hour average wind speeds were used.

Afternoon averages were then used; the rationale being that it is usually the warm afternoon winds that bring dry and hot air in the form of horizontal sensible heat flux into the local vertical exchange of fluxes and therefore affecting the accuracy of the model since it defies the EF assumption. When afternoon average wind speeds were used, instead of 24-hour averages, there was more distinction in the performance of the model between calm and windy

conditions. The calm conditions resulted in MBE of only  $-0.9 \text{ mm d}^{-1}$  (-12%), while winds exceeding  $2 \text{ m s}^{-1}$  resulted in error of  $-4.7 \text{ mm d}^{-1}$  (-43%).

When considering the vegetation cover, there seemed to be not much difference in alfalfa ET between less vegetated (MBE =  $-2.2 \text{ mm d}^{-1}$ , -35%) and more vegetated (MBE =  $-2.9 \text{ mm d}^{-1}$ , -31%) surface. An LAI between 1.0 and  $4.0 \text{ m}^2 \text{ m}^{-2}$  was regarded as “less vegetated”, and LAI greater than  $4.0 \text{ m}^2 \text{ m}^{-2}$  was considered “more vegetated”. Field conditions with LAI less than 1.0 were not used.

While there is also a difference observed between the calm and windy conditions in METRIC, it is not as much as in SEBAL. This could be because of the ability of the METRIC model to better account for advection, using the Penman Monteith alfalfa reference ET. However, it seems that while METRIC seems to better account for advection, it does not entirely do so; hence there is still an increase in error with increasing wind speed. As observed with SEBAL, when using the afternoon wind averages, the influence of wind becomes more apparent.

When comparing the different vegetation covers, METRIC is more accurate in the estimation of ET when there is more cover than when there is less. This is an expected observation as there is more error associated with low biomass as earlier discussed. The reason such was not observed in SEBAL could be that the well-vegetated surfaces also had error due to advection, and advection would have less effect on surfaces with low biomass.

### **Effects of humidity on SEBAL model performance**

Table 1.4 shows results from the SEBAL model, indicating that there was less error on days when the average relative humidity was close and above 70 %. On days 15 June 2010, 10 August 2010 and 5 August 2011, when the humidity was high, the errors on ET were less than

10%. However on low humidity days (e.g. 6 May 2010, 22 May 2010, 20 June 2012 and 22 July 2012) when the average relative humidity was less than 45%, for example, the error was consistently above 30% and reaching up to 50%, when low humidity was accompanied by higher wind speed. This is in agreement with Gentine et al. (2011) that under conditions of higher relative humidity, the evaporative fraction is more likely to be constant, and therefore the extrapolation of instantaneous ET to daily ET would be more accurate,

From the discussion above, the influence of humidity, temperature and wind; parameters, which De Bruin et al. (2005) termed advection indicators, was observed on the accuracy of the SEBAL model. However, there is still complexity as to how these indicators interact with each other and also with the evaporating surface in order to determine how much latent heat flux is due to the advected energy. Table 1.4 shows various examples of the interactions.

For instance, 22 May 2010 was the day with the highest ET overestimation observed, in both fields A and B. From analysis of the weather data, also shown in Table 1.4, this was due to the high wind speed of 3-4 m s<sup>-1</sup> and a low relative humidity of 30%. This resulted in SEBAL underestimating ET by 45% and 51% for fields A and B, respectively. The opposite occurs on 10 August 2010, where there was no error in ET estimation, and the conditions prevailing were non-advective, with the average wind speed being 0.9 m s<sup>-1</sup> and a relative humidity of 69 %.

On the 26<sup>th</sup> August 2010, SEBAL overestimated ET by 28 %. Weather conditions would suggest some presence of advection, though slight, which should have resulted in a slight underestimation of ET. This result could be explained by the fact that the alfalfa in the field was only about 12 cm tall, with low biomass and sparse cover. The performance of SEBAL and METRIC under such conditions was inaccurate as has been explained earlier.

On 4 July 2011, the 24-hour average wind speed was low ( $1.1 \text{ m s}^{-1}$ ) and RH of about 50%, but the SEBAL model underestimated ET by 33%. This observation shows that the 24-hour average wind speed may not be a good indicator of advection as was discussed earlier, as Table 1.4 shows that the afternoon average wind speed was  $2.7 \text{ m s}^{-1}$ , and therefore capable of transporting substantial sensible heat from surrounding areas. Similar observation was made on 22 July 2012 in field A, where a 49% underestimation of ET by SEBAL was observed, with a 24-hour average wind speed of  $1.6 \text{ m s}^{-1}$ . However, the afternoon average wind speed was  $2.8 \text{ m s}^{-1}$ , and afternoon average temperature and RH were  $34^{\circ}\text{C}$  and 24% respectively which suggest advective conditions.

The day of 6 May 2010 was a windy day, especially in the afternoon with an average wind speed of  $8.4 \text{ m s}^{-1}$ , but the ET error was less than 30% in Field A, which was less than other days with low wind speed and higher RH. This could have been due to the lower temperatures on the day compared to the other days, with mean temperature being  $16.2^{\circ}\text{C}$ , thus the air brought onto the field was cool and therefore had less sensible heat energy.

Table 1.4 also shows that on advective days, there is some evapotranspiration that occurs in the absence of solar radiation (late afternoon and night). For example on 22 May 2010 in field B, about 2.1 mm was recorded when there was no solar radiation measured, so it was only the sensible heat that was responsible for this amount of ET. On non-advective days, there is usually no ET during the night, e.g. 10 August 2010 in the field A, which suggests that the ET on that day was only due to vertical exchange of energy.

## CONCLUSIONS

From the results obtained from the study, it can be concluded that the SEBAL model usually underestimates ET mostly due to advection, with bias errors of up to 50 % being observed. The daily ET had more error than the hourly ET, because advection in Rocky Ford, Colorado occurs mostly in the afternoons, while hourly ET is estimated around the satellite overpass time, which is between 10:20 a.m. and 10:30 a.m. Mountain Standard Time (MST).

METRIC performed better than SEBAL, with less error especially under conditions of advection. This was due to the former model's capacity to better account for advection, by using the  $ET_rF$  function. However, there was evidence in the analyzed data, that even METRIC was not able to fully account for advection, as there was still considerable error in daily ET with windy than calm conditions. In SEBAL, the error was strongly linked to the assumption of constant EF, such that when  $EF_{24}$  was related to SEBAL alfalfa daily ET bias error (%), the  $R^2$  equaled 0.98, as shown in Figure 1.9.

It was also observed that the models estimated ET more accurately when there was more vegetation cover. There are several possible explanations to these observations. One is that the models used in this study are single-source models, assuming that all the fluxes are from a single uniform source (big leaf approach). However with low cover, where the soil is exposed, a two-source approach is theoretically more accurate and appropriate. Another reason for higher accuracy with full vegetation cover is that H is usually small, and therefore even if H is inaccurately estimated, it will have less impact on the final LE value. However, with low cover fields, and/or water stressed fields, both G and H may be large and errors in its determination may significantly affect the accuracy of LE as a residual of the surface energy balance. The estimation of H involves the selection of extreme pixels, which is a subjective exercise, and

depends on several factors, which include the presence of appropriate pixels and also the experience of the person processing the image.

Figures 1.9-1.11 show a strong relationship between wind speed (an advection indicator) and alfalfa daily ET error resulting from applying SEBAL, with stronger winds resulting in larger ET error. The afternoon average wind speeds had the strongest relationship with errors in daily ET ( $R^2 = 0.97$ ), followed by a somewhat weaker relationship with daytime average wind speed ( $R^2 = 0.89$ ), and by an even weaker relationship for 24-hour average wind speed ( $R^2 = 0.83$ ). This finding made sense because afternoon winds, in general, are higher and may transport more sensible heat energy, as the air is often warmer and relatively dry.

## **RECOMMENDATIONS**

1. It is recommended that in semi-arid and arid areas, the METRIC ET algorithm be used instead of SEBAL since it better accounts for advected energy than SEBAL. The use of SEBAL to estimate daily ET of irrigated areas in semi-arid and arid regions, subject to advection, may not be appropriate and may result in underestimation of ET.
2. It is recommended that a new RS model be developed that will account for advection while requiring minimal weather data.

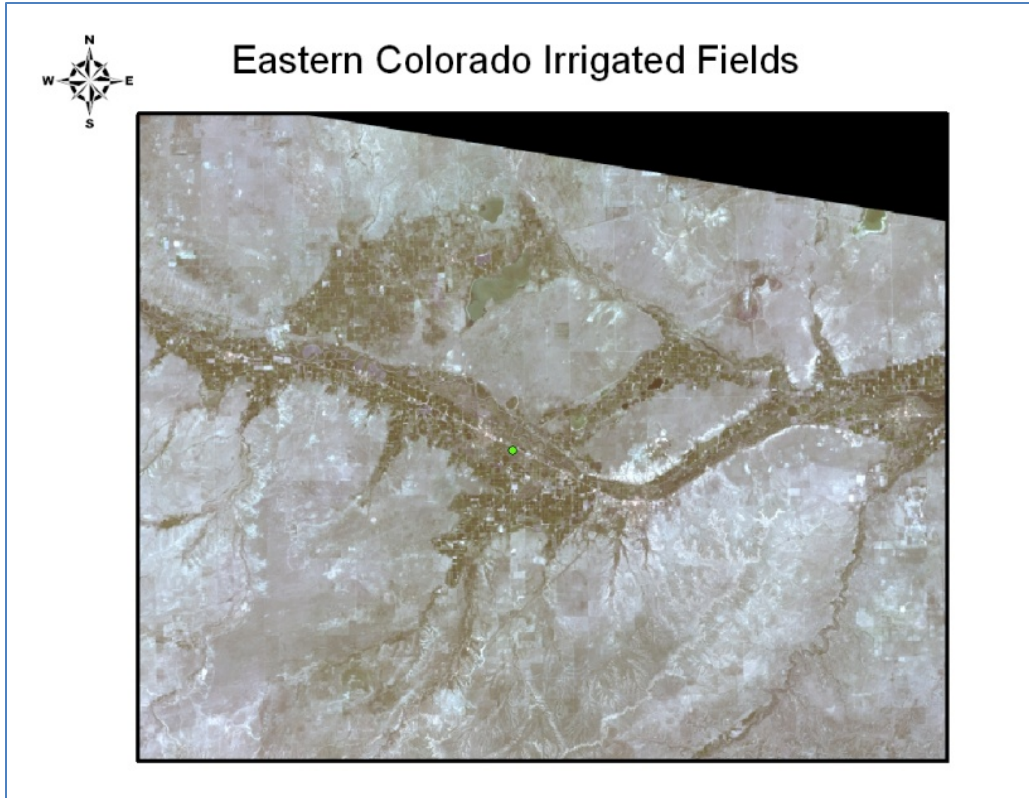


Figure 1.1: Study area, irrigated fields surrounded by dry areas

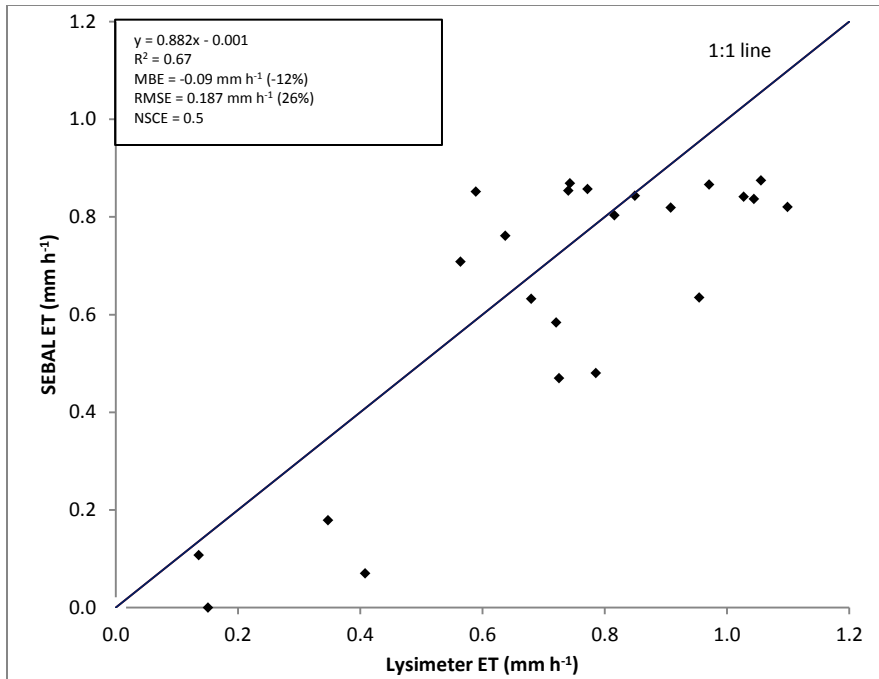


Figure 1.2: Comparing SEBAL-modeled and Lysimeter-measured hourly alfalfa ET

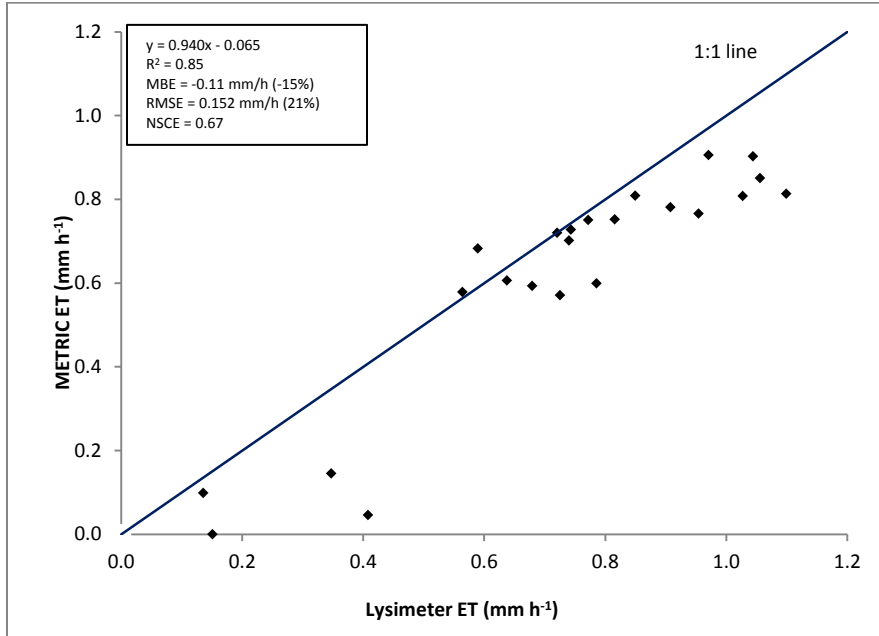


Figure 1.3: Comparing METRIC-modeled and Lysimeter-measured hourly alfalfa ET

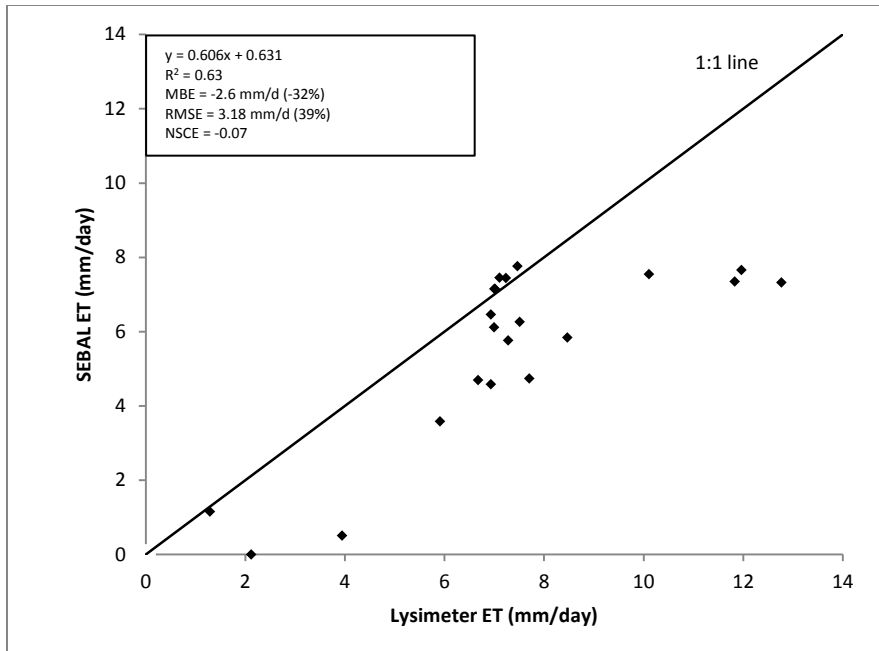


Figure 4: Comparing SEBAL-modeled and Lysimeter-measured daily alfalfa ET

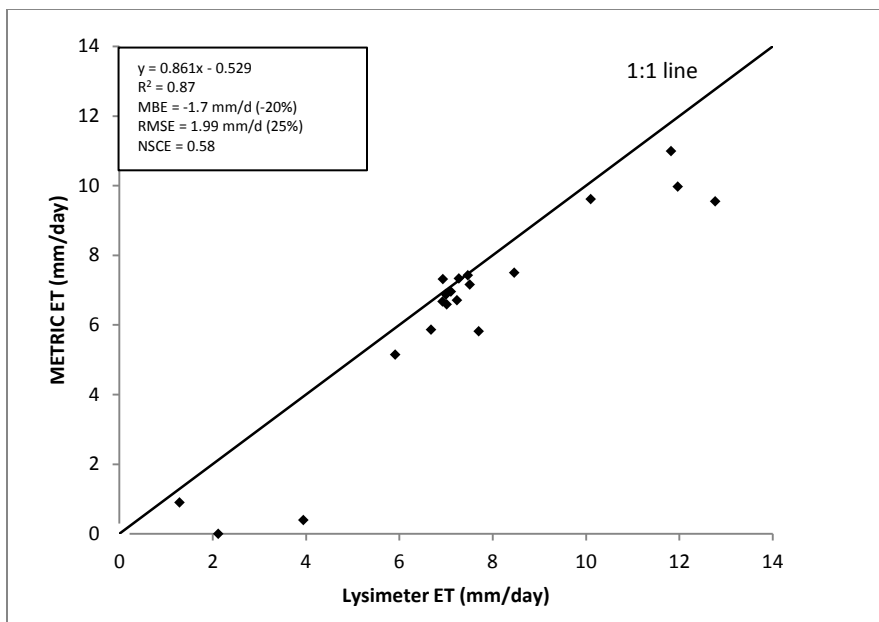


Figure 1.5: Comparing METRIC-modeled and Lysimeter-measured alfalfa daily ET

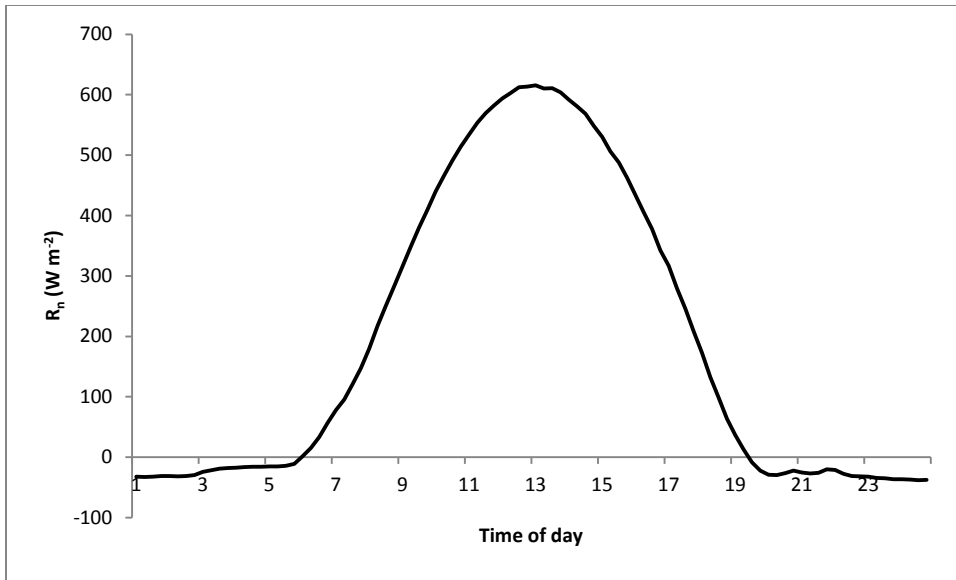


Figure 1.6: Daily Pattern of net radiation measured on a cloud-free day, 7/29/2010.

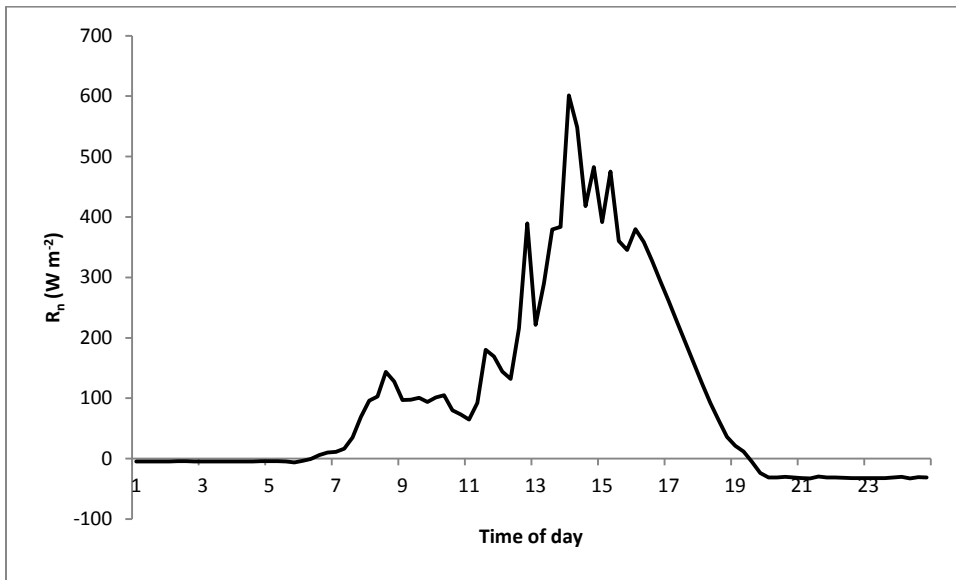


Figure 1.7: Daily Pattern of measured net radiation on a cloudy day, 08/15/2010.

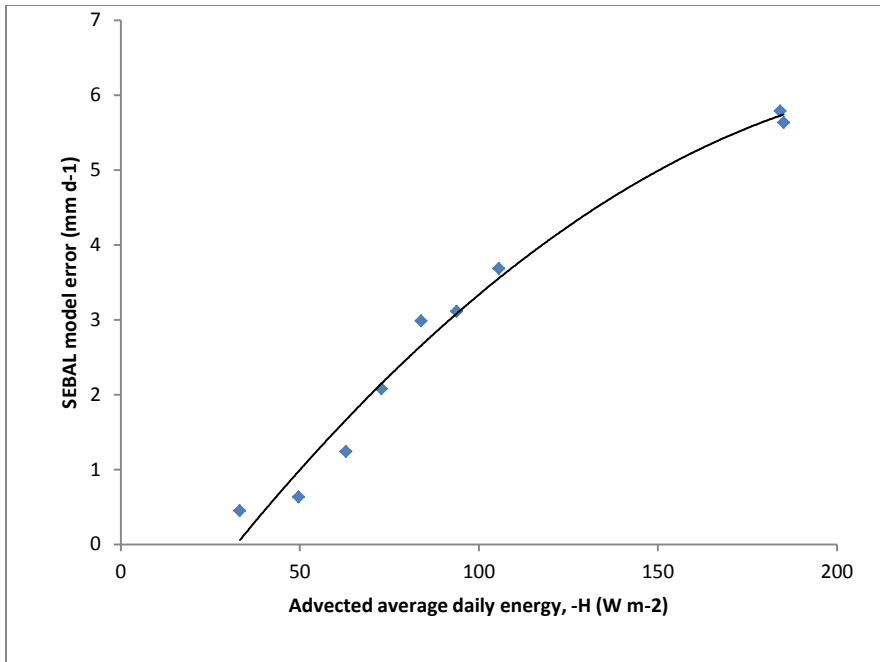


Figure 1.8: Relationship between advected energy and SEBAL error on daily alfalfa ET

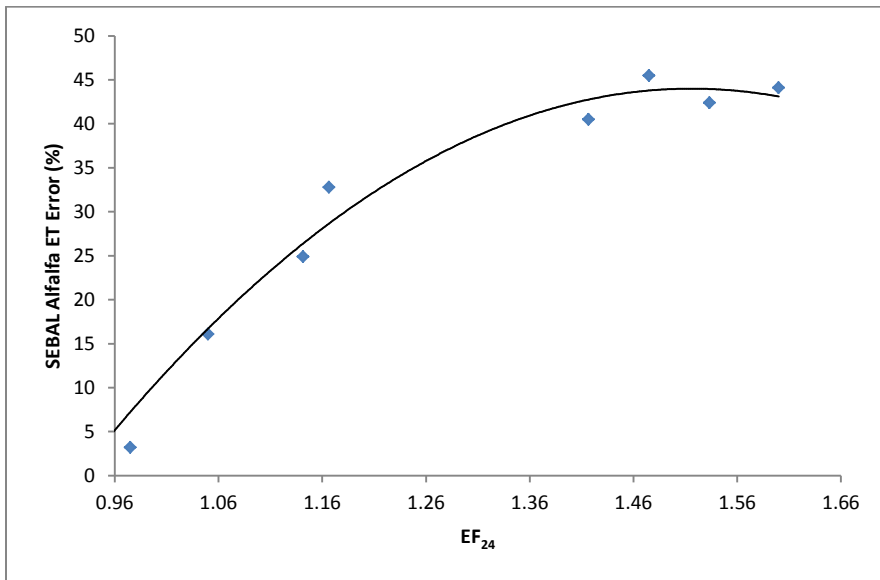


Figure 1.9: Relationship between average daily EF and % error in estimating daily alfalfa ET

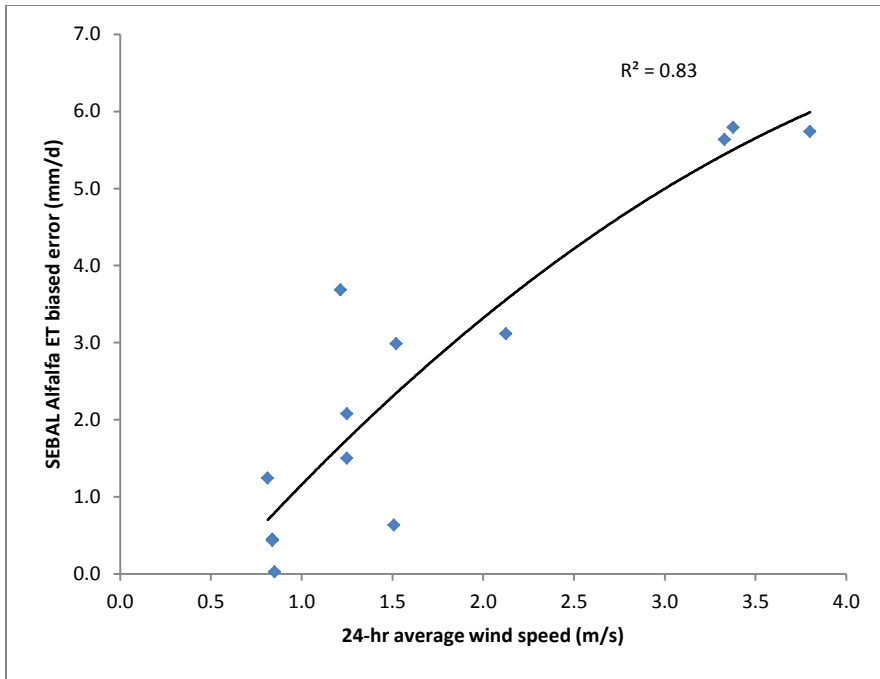


Figure 1.10: Relationship between 24-hr average wind speed and SEBAL model alfalfa ET error

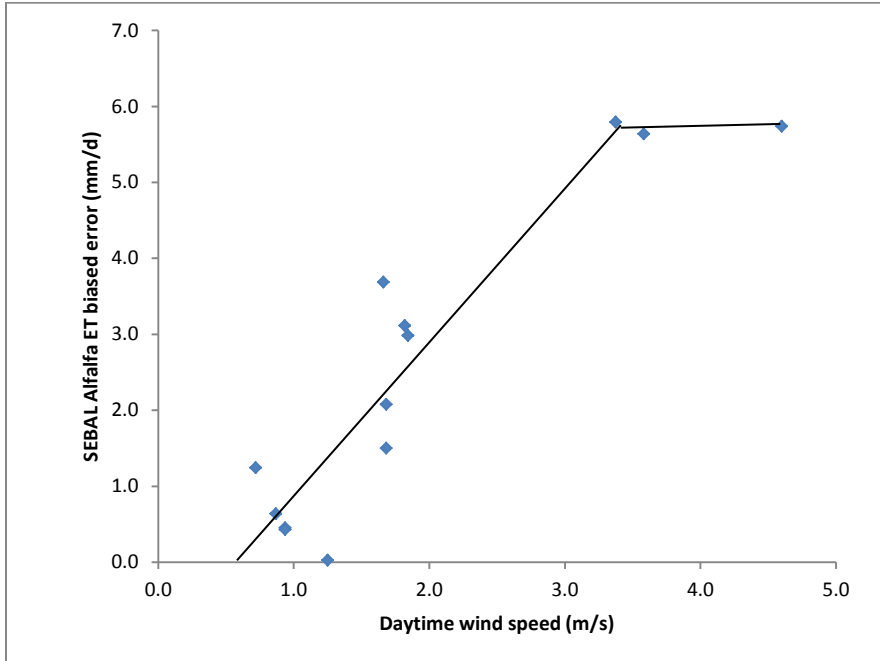


Figure 1.11: Relationship between daytime average wind speed and SEBAL model alfalfa ET error

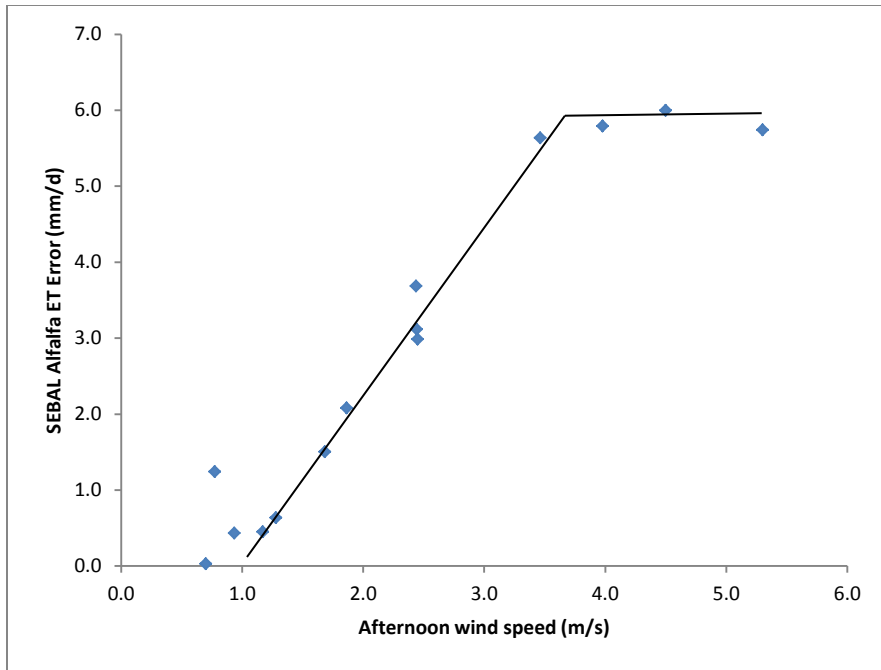


Figure 1.12: Relationship between afternoon wind speed averages and SEBAL alfalfa ET model error

Table 1.1: Equations relating NDVI and radiometric surface temperature

Date	Equation	RMSE/ $\sigma$
05/22/10	$y = -23.452x + 319.05$	0.19
06/15/10	$y = -17.154x + 311.00$	0.11
07/01/10	$y = -23.876x + 319.45$	0.26
08/02/10	$y = -15.605x + 312.90$	0.23
08/10/10	$y = -19.177x + 314.49$	0.18
08/18/10	$y = -22.060x + 317.92$	0.28
08/26/10	$y = -32.753x + 323.80$	0.36
09/11/10	$y = -24.861x + 314.51$	0.18
09/19/10	$y = -20.691x + 313.14$	0.10
09/27/10	$y = -24.191x + 317.78$	0.18
10/05/10	$y = -17.892x + 309.36$	0.35
08/05/11	$y = -20.854x + 315.94$	0.19
08/21/11	$y = -21.436x + 315.84$	0.15
09/22/11	$y = -12.254x + 303.48$	0.42

Table 1.2: Performance indicators for SEBAL under varying wind and vegetation cover conditions

	MBE	RMSE	NSCE
<b>24 hour wind speed</b>			
0 – 2 m s <sup>-1</sup>	-1.40 mm d <sup>-1</sup> (-17%)	1.79 mm d <sup>-1</sup> (22%)	-1.48
>2 m s <sup>-1</sup>	-3.81 mm d <sup>-1</sup> (-40%)	4.02 mm d <sup>-1</sup> (42%)	-2.08
<b>Afternoon winds</b>			
0 – 2 m s <sup>-1</sup>	-0.91 mm d <sup>-1</sup> (-12%)	1.13 mm d <sup>-1</sup> (15%)	-5.60
>2 m s <sup>-1</sup>	-4.7 mm d <sup>-1</sup> (-43%)	4.9 mm d <sup>-1</sup> (45%)	-1.86
<b>Vegetation cover</b>			
LAI < 4.0 m <sup>2</sup> m <sup>-2</sup>	-2.24 mm d <sup>-1</sup> (-35%)	2.62 mm d <sup>-1</sup> (41%)	0.1
LAI > 4.0 m <sup>2</sup> m <sup>-2</sup>	-2.9 mm d <sup>-1</sup> (-31%)	3.59 mm d <sup>-1</sup> (38%)	-0.3

Table 1.3: Performance indicators for METRIC under varying wind and vegetation cover conditions

	<b>MBE</b>	<b>RMSE</b>	<b>NSCE</b>
<b>24 hour winds</b>			
0 – 2 m s <sup>-1</sup>	-1.03 mm d <sup>-1</sup> (-13%)	1.08 mm d <sup>-1</sup> (22%)	0.10
>2 m s <sup>-1</sup>	-1.88 mm d <sup>-1</sup> (-20%)	2.05 mm d <sup>-1</sup> (21%)	0.24
<b>Afternoon winds</b>			
0 – 2 m s <sup>-1</sup>	-0.89 mm d <sup>-1</sup> (-11%)	0.93 mm d <sup>-1</sup> (12%)	-8.57
>2 m s <sup>-1</sup>	-2.13 mm d <sup>-1</sup> (-20%)	2.30 mm d <sup>-1</sup> (22%)	0.4
<b>Vegetation cover</b>			
LAI < 4.0 m <sup>2</sup> m <sup>-2</sup>	-1.85 mm d <sup>-1</sup> (-29%)	2.16 mm d <sup>-1</sup> (38%)	0.38
LAI > 4.0 m <sup>2</sup> m <sup>-2</sup>	-1.63 mm d <sup>-1</sup> (-18%)	2.02 mm d <sup>-1</sup> (34%)	0.59

Table 1.4: Average weather conditions, field measurements and model performance on days of satellite overpass

<b>Date</b>	<b>T<sub>a</sub> (°C)</b>	<b>RH (%)</b>	<b>U (m s<sup>-1</sup>)</b>		<b>h<sub>c</sub> (cm)</b>	<b>Model error (%)</b>	<b>Night ET</b>
			<b>24-hr</b>	<b>Afternoon</b>			
6/15/2010 (A)	19.2	66.7	1.4	3.2	30	-7.7	0.4
7/1/2010 (A)	24.8	47.7	3.3	3.7	66	-44.3	1.1
8/18/2010 (A)	24.3	55.5	0.8	0.9	55	-16.7	0.4
5/6/2010 (A)	16.2	40.7	4.3	8.4	43	-29.0	0.7
5/22/2010 (A)	23.2	28	3.8	5.3	60	-45.0	1.4
8/10/2010 (A)	23.0	69.1	0.9	1.0	50	0.0	0.0
8/26/2010 (A)	22.1	46.6	1.8	2.6	12	27.6	0.4
6/15/2010 (B)	18.8	70.1	1.4	2.5	104	-3.7	0.2
5/6/2010 (B)	15.7	42.9	3.6	6.8	60	-32.7	1.0
5/22/2010 (B)	22.1	32.3	3.0	4.0	92	-50.6	2.1
8/10/2010 (B)	23.7	63.5	1.0	1.0	*	-13.6	0.2
6/18/2011 (A)	22.1	50	2.4	3.7	25	-28.4	0.5
7/4/2011 (A)	24.4	49.8	1.1	2.7	70	-33.0	0.1
8/21/2011 (A)	23.7	62.9	1.3	1.7	70	-24.1	0.3
6/18/2011 (B)	22.2	50.3	2.4	3.5	18	-44.0	0.7
8/5/2011 (B)	23.9	64.3	0.9	0.9	48	-6.3	0.6
6/4/2012 (B)	22.6	46.6	2.7	5.2	25	-35.6	0.4
6/4/2012 (A)	22.4	47.7	2.8	5.6	32	-37.9	0.6
6/20/2012 (A)	23.1	43.6	3.4	3.5	76	-42.1	1.7
7/22/2012 (A)	27.0	36.4	1.6	2.8	53	-48.6	1.1

Note: T<sub>a</sub> is air temperature, U is the wind speed, RH is relative humidity and h<sub>c</sub> is the crop height.

## REFERENCES

Agam N, Kustas WP, Anderson MC, Li Fuqin, Colaizzi PD (2008) Utility of thermal image sharpening for monitoring field-scale evapotranspiration over rainfed and irrigated agricultural regions. *Geographical Research Letters*, Vol. 35.

Allen RG, Pereira LS, Raes D, Smith M (1998) Crop Evapotranspiration: Guidelines for computing crop water requirements, FAO Irrigation and Drainage Paper No. 56. Food and Agriculture Organization, Land and Water. Rome, Italy.

Allen RG, Tasumi M, Morse A, Trezza R (2005) Satellite-based evapotranspiration by energy balance for western states water management. Presented at the US Bureau of Reclamation evapotranspiration workshop. Feb 8-10, 2005.

Allen RG, Tasumi M, Trezza R (2007) Satellite-based energy balance for mapping evapotranspiration with internalized calibration (METRIC) model. *ASCE J Irrig Drain Eng* 133(4):380-394.

Allen RG, Robison CW, Garcia M, Kjaersgaard J (2008) Enhanced resolution of evapotranspiration by sharpening the Landsat thermal band. Pecora 17 – The Future of Land Imaging..Going Operational. November 18-20, 2008. Denver, Colorado.

Allen R, Irmak A, Trezza R, Hendrickx JMH, Bastiaanssen W, Kjaersgaard J (2011) Satellite-based ET estimation in agriculture using SEBAL and METRIC. *Hydrol. Process.* 25, 4011-4027.

Badeck FW, Bondeau A, Bottcher K, Doktor D, Lucht W, Schaber J, Sitch S (2004) Responses of spring phenology to climate change. *New Phytol.* 162:295-309.

Bastiaanssen WGM (1995) Regionalization of surface flux densities and moisture indicators in composite terrain: A remote sensing approach under clear skies in Mediterranean climates. *PhD. Dissertation*, CIP Data Koninklijke Bibliotheek, Den Haag, The Netherlands, 273p.

Bastiaanssen WGM, Menenti M, Feddes RA and Holtslag AAM (1998) Remote sensing surface energy balance algorithm for land (SEBAL): 1. Formulation. *J. Hydrol.*, 212-213(1-4), 198-212.

Bastiaanssen WGM, Noordman EJM, Pelgrum H, Davids G, Thoreson BP, Allen RG (2005) SEBAL Model with remotely sensed data to improve water resources management under actual field conditions. *Journal of Irrigation and Drainage Engineering*, 131 (1):85-93.

Brakke TW, Verma SB, Rosenberg NJ (1978) Local and Regional Components of Sensible Heat Advection. American Meteorological Society. Paper No. 5428.

Challinor A, Wheeler T, Garforth C, Cranford P, and Kassam A (2005) Assessing the vulnerability of food crop systems in Africa to climate change. *Climate Change*. 83: 381-399.

Chávez JL, Neale CMU, Hipps LE, Prueger JH, Kustas WP (2005) Comparing aircraft-based remotely sensed energy balance fluxes with eddy covariance tower data using heat flux source area functions. *J. of Hydrometeorology*, AMS. 6 (6): 923-940.

Chávez JL, Gowda PH, Howell TA, Neale CMU, Copeland KS (2009) Estimating hourly crop ET using a two-source energy balance model and multispectral airborne imagery. *Irrigation Science Journal* 38:79-91.

Chávez JL, Howell TA, Gowda PH, Copeland KS, Prueger JH (2010) Surface aerodynamic temperature modeling over rainfed cotton. *American Society of Agricultural and Biological Engineers*. 53(3): 759-767.

Crago RD and Brutsaert W (1996) Daytime evaporation and the self-preservation of the evaporative fraction and the Bowen ratio. *J. Hydrol.*, 178, 241-255.

De Bruin HAR, Hartogensis OK, Allen RG, Kramer JWJL (2005) Regional Advection Perturbations in an Irrigated Desert (RAPID) experiment. *Theor. Appl. Climatol.* 80, 143-152.

Elhaddad A and Garcia LA (2008) Surface energy balance-based model for estimating evapotranspiration taking into account spatial variability in weather. *Journal of Irrigation and Drainage Engineering*, 134 (6):681-689.

Gentine P, Entekhabi D, Chehbouni A, Polcher J (2011) The diurnal behavior of evaporative fraction in the soil-vegetation-atmospheric boundary layer continuum. *Journal of Hydrometeorology*, Vol. 12. 1530-1546.

Gowda PH, Chavez JL, Colaizzi PD, Evett SR, Howell TA, Tolk AT (2008) ET mapping for agricultural water management: present status and challenges. *Irrigation Science.* 26: 223-237.

Gowda PH, Howell TA, Paul G, Colaizzi PD, Marek TH (2011) SEBAL for estimating hourly ET fluxes over irrigated and dryland cotton during BEAREX08. World Environmental and Water Resources Congress. ASCE.

Hippias L, Kustas W (2000) Patterns and organisation in Evaporation, in *Spatial Patterns in Hydrological Processes: Observations and Modelling*, edited by RB Grayson and G Biöschl, pp. 105-122, Cambridge University Press, New York.

Karnieli A, Bayasgalan M, Bayarjargal Y, Agam N, Khudulmur S, Tucker CJ (2006) Comments on the use of the vegetation health index over Mongolia. *Int. J. Remote Sens.* 27:2017-2024.

Katiyar AK, Kumar A, Kumar Pandey C, Das b (2010) A comparative study of monthly mean daily clear sky radiation over India. *International Journal of Energy and Environment*. 1(1): 177-182.

Kustas WP and Norman JM (2000) Evaluating the effects of sub-pixel heterogeneity on pixel average fluxes. *Remote Sensing of Environ.* 74:327-342.

Lhomme JP and Elguero E (1999) Examination of evaporative fraction diurnal behavior using a soil-vegetation model coupled with a mixed-layer model. *Hydrology and Earth System Sciences*, 3(2):259-270.

Li F and Lyons TJ (1999) Estimation of Regional Evapotranspiration through remote sensing. *J. Appl. Meteor.* 38: 1644-1654.

Moriasi DN, Arnold JG, Van Liew MW, Bingner RL, Harmel RD, Veith TL (2007) Model evaluation guidelines for systematic quantification of accuracy in watershed simulations, *Trans. ASABE*, 50(3): 885-900.

Nash JE and Sutcliffe JV (1970) River flow forecasting through conceptual models part 1- A discussion of principles. *Journal of Hydrology*, 10 (3): 282-290.

Nichols WE and Cuenca RH (1993) Evaluation of the evaporative fraction for parameterization of the surface energy balance. *Wat. Resour. Res.*, 29, 3681-3690.

Paul G, Gowda PH, Vara Prasad PV, Howell TA, Staggenborg SA (2011) Evaluating surface energy balance system (SEBS) using aircraft data collected during BEAREX07. *World Environmental and Water Resources Congress: Bearing knowledge for Sustainability*. ASCE.

Shuttleworth JW and Wallace JS (1985) Evaporation of sparse crops – an energy combination theory. *Quarterly Journal of the Royal Meteorological Society*, Vol. III, pp 839-885. January.

Singh RK, Irmak A, Irmak S, Martin DL (2008) Application of SEBAL Model for mapping evapotranspiration and estimating surface energy fluxes in South-Central Nebraska. *Journal of Irrigation and Drainage Engineering*, 134 (3): 273-285.

Suleiman AA, Bali KM, Kleissl J (2009) Comparison of ALARM and SEBAL Evapotranspiration of Irrigated Alfalfa. 2009 ASABE Annual International Meeting.

Trezza R (2002) Evapotranspiration using a satellite-based surface energy balance with standardized ground control. *PhD Dissertation*, Biological and Irrigation Engineering Department, Utah State University, Logan.

Wilmott CJ (1982) Some comments on the evaluation of model performance. *Bulleting American of Meteorological Society*, 63 (11): 1309-1313.

Wonsook H, Gowda PH, Howell TA, Paul G, Hernandez JE, Basu S (2010) Downscaling surface temperature image with TsHARP. ASABE Conference Proceedings, 5-8 December, 2010. Phoenix, Arizona.

Zermeño-Gonzalez A and Hippias LE (1997) Downwind evolution of surface fluxes over a vegetated surface during local advection of heat and saturation deficit. *Journal of Hydrology* 192: 189-210.

## CHAPTER 2

### **Modifying SEBAL RS of ET algorithm: Accounting for advection**

#### **Overview**

The Surface Energy Balance Algorithm for Land (SEBAL) is one of the remote sensing (RS) models that are increasingly being used for evapotranspiration (ET) determination. It is a widely used model mainly due to the fact that it requires minimum weather data and no prior knowledge of surface characteristics is needed. However, it underestimates ET under advective conditions because it regards net radiation as the only energy available for evaporation. A modified SEBAL model, which uses minimal weather data to estimate advection, was developed in this study. An advection component, which is absent in the original SEBAL, was introduced such that the energy available for evapotranspiration was a sum of net radiation and advected heat energy.

The model was developed and tested in Rocky Ford in southeastern Colorado, a semi-arid area where afternoon advection is a common feature. In this study, the SEBAL model was modified for standard surface conditions, which are described as healthy alfalfa with height of 40-60 cm, without water-stress. ET values estimated using the original and modified SEBAL were compared to large weighing lysimeter-measured ET values. When the modified SEBAL ET was compared with the original SEBAL ET values, the results were improved, with the ET Mean Bias Error (MBE) reduced from -17.1 % to 2.2 % and the Root Mean Square Error (RMSE) reduced from 25.1 % to 10.9 %. It was therefore concluded that the modified SEBAL model is suitable for arid and semi-arid regions where there is advection. It was also recommended that the developed model be tested on non-standard surfaces.

## INTRODUCTION

Remote sensing (RS) models estimate instantaneous ET ( $ET_{inst}$ ), and use various extrapolation methods to determine ET for longer time-steps (e.g. hourly, daily and seasonal). In most cases, the daily and seasonal ET values are more important than ET for the short time steps, e.g. 15-minute or hourly. It is therefore crucial that the methods employed to extrapolate  $ET_{inst}$  to daily, and eventually to seasonal ET be accurate. Inaccuracies in some RS methods have in some cases been due to assumptions made in the extrapolation of  $ET_{inst}$  to daily and subsequently seasonal ET. This chapter focused on the extrapolation to daily ET, analyzing the approach used in SEBAL.

SEBAL uses the evaporative fraction (EF) to determine the 24-hour ET ( $ET_{24}$ ). This EF is defined as the ratio of latent heat flux (LE) to available energy (AE), where AE is net radiation less soil heat flux ( $R_n - G$ ). This ratio is assumed to be constant throughout the day (Hoedjes et al., 2008). This assumption in the EF approach results in  $ET_{24}$  underestimation on days when there is advection (Allen et al., 2005; Singh et al., 2008). The Mapping Evapotranspiration with Internalized Calibration (METRIC) model on the other hand, uses the fraction of alfalfa reference ET ( $ET_rF$ ) which is the ratio of the actual crop (vegetation) ET to alfalfa reference ET.

The  $ET_rF$  is also assumed to be constant throughout the day and yet capable of capturing the effects of advection. However, the  $ET_rF$  function requires hourly weather data, which makes this approach unsuitable for places where weather data at such short time steps is unavailable, e.g. in many developing countries.

In Chapter 1, errors of up to 40 % were observed on days of advection characterized by higher wind speed, and warm and dry air. A Nash-Sutcliffe coefficient efficiency value of -0.07 was obtained when comparing SEBAL estimated ET with lysimeter-measured ET. This indicates

that SEBAL is not suitable to estimate ET in areas where there is advection. The error may be compounded if the EF obtained at the time of satellite overpass is also not accurate. As explained in Chapter 1, SEBAL assumes that at the cold pixel, the sensible heat flux (H) is zero. This may not be the case when there is advection at the time of overpass, where H may be negative for well-irrigated crops, in which case the EF is supposed to be larger than unity. However, preliminary work at Rocky Ford suggested that advective conditions are unlikely in this area at time of satellite overpass, which is between 10:20 am and 10:30 am Mountain Standard Time (MST). When EF was determined for irrigated alfalfa using H obtained from METRIC (which better incorporates the effects of advection at time of overpass) and  $R_n$  and G, the EF exceeded unity only a few times, and only slightly with the highest EF value being 1.1. This means that much of the SEBAL error was due to advection that took place in the afternoon, and not at time of satellite overpass.

An alternative model that is used to model ET under advective conditions is METRIC. However, this model requires several weather variables to be observed at short time steps (e.g., hourly), which requires automatic weather stations, which some developing countries do not have. These areas would only have daily averages of most weather variables. It was therefore recommended that a modified SEBAL model be developed that would account for advection while requiring minimal weather data.

### **EF constancy throughout the day**

The characteristic of EF being constant throughout the day has been supported in several publications; Brutsaert and Sugita (1992), Crago and Brutsaert (1996), Bastiaanssen et al. (2005). However Stewart (1996), as cited in Lhomme and Elguero (1999) mentions that the

simplification of assuming that EF is constant throughout the day may be erroneous. In his study, he concluded that even in fair weather EF has a typical concave shape during the day, with the EF values in central hours around solar noon lower than the daytime average. According to the study, factors like soil water content, incoming shortwave energy, and vapor pressure deficit influence the EF constancy.

Gentine et al. (2011) agreed that although EF may be constant for high values of relative humidity (75-90 %), for  $RH < 50 \%$ , it has a noticeable parabolic shape. This means that a constant EF may apply in humid but not in arid or semi-arid regions. Suleiman et al. (2009) on a particular day in Blythe, California, found EF to be fairly constant at 1.08 from 7 am to 2 pm then he showed that EF started increasing until it reached 1.35 by 7 pm. Lhomme and Elguero (1999) state that EF taken about 3 hours before or after solar noon could best represent the daily average EF. Non-constancy of diurnal EF, as stated by Lhomme and Elguero (1999) has been observed under calm conditions, worse results may be observed under conditions of advection.

In Rocky Ford, southeastern Colorado, the EF was calculated based on  $R_n$ ,  $G$  and  $ET$  measured with sensors from the experimental field planted to alfalfa. On one advective day (22 May 2010), EF was found to vary throughout the day. It was above 1 in the morning, dropping to 1 around mid-day, then rising in the afternoon, and larger than 2 in the late afternoon. Figure 2.1 shows the EF variation over the day. The EF values in the late afternoon seem too large because of the net radiation being close to zero at that time of the day while the warm air was still supplying energy (horizontally) for evapotranspiration.

Hoedges et al. (2008) observed that EF would remain fairly constant under dry surface conditions, but not under wet or moist conditions; and since wet conditions result in higher  $ET$

rates, assuming a constant EF value would therefore result in large errors of daily ET estimation from well-watered fields.

There are various methods proposed in the literature to adjust for the error caused by the assumption of a constant EF. One of the methods involves establishing a relationship between  $EF_{inst}$  and the daylight average EF as suggested by Shuttleworth et al. (1989). They carried out an experiment in homogenous grassland and found that midday EF is nearly equal to the average daylight EF. Nichols and Cuenca (1993) found that the midday EF was highly correlated with the average daytime EF but not necessarily the same value. Farah et al. (2004) when relating instantaneous measurements of EF to average day EF found the diurnal variability of EF to be complex as EF was found to be a function of several factors such as available energy ( $R_n - G$ ), vapor pressure deficit (VPD), surface resistance to water vapor transport ( $r_s$ ) and aerodynamic resistance to heat transport ( $r_{ah}$ ).

## **Objectives**

The objective of this chapter was to develop a modified version of SEBAL that accounts for advection by using minimum available weather data. The method adopted in this study used a semi-empirical approach to estimate advected energy, and then incorporated the estimated advection into the  $ET_{24}$  sub-model of SEBAL.

## **MATERIALS AND METHODS**

### **Study Area**

The research was carried out at Colorado State University (CSU) Arkansas Valley Research Center (AVRC) near Rocky Ford, in southeastern Colorado. The study area has

geographic coordinates 38° 02' N, 103° 41' W, with an elevation of 1,274 m above mean sea level (amsl). The rainfall received annually in the area averages about 300 mm, with 65% falling in May through September. This amount of rainfall is not enough to sustain most agricultural crops, which makes irrigation necessary. Dry areas surround the irrigated fields as the region is of a semi-arid nature. The temperature in summer averages 23.6 °C, with an average daily maximum of 33 °C. The average relative humidity in the mid-afternoon is 25 % in summer, and average wind speed is 4.4 m s<sup>-1</sup>. All these conditions make afternoon advection in the area to be a common occurrence.

Two fields were used for the study, both planted to alfalfa which was irrigated using a furrow irrigation system supplied by siphons and a head ditch. Field A was rectangular, 160 m by 250 m, and field B was triangular (right-angled, with side 110 m and perpendicular length of 230 m). Close to the center of field A was a large monolith weighing lysimeter (3 m × 3 m × 2.4 m deep), and a smaller lysimeter (1.5 m × 1.5 m × 2.4 m deep) was in Field B. Both fields were equipped with net radiometers (REBS, Campbell Scientific International (CSI), Logan, Utah, U.S.A.). There were also infrared thermometers (IRT, Apogee model S1-111, CSI, Logan, Utah, U.S.A.) to measure crop radiometric surface temperature. Soil heat flux plates (REBS model HFT3, CSI, Logan, Utah, U.S.A.) were buried 10 cm in the ground, along with soil temperature and soil volumetric water content sensors at locations near the net radiometer with their measurements used in the calculation of soil heat flux.

### **Landsat Satellite Datasets and Processing**

Landsat 5 Thematic Mapper (TM) and Landsat 7 Enhanced Thematic Mapper Plus (ETM+) satellite images were downloaded from the USGS Earth Explorer site [<http://edcsns17.cr.usgs.gov/NewEarthExplorer/>] for the 2010-2012 growing seasons. The

temporal resolution (or revisit period) is 16 days for both satellites, with alternating coverage. Therefore if cloud cover or the swaths of missing data for Landsat 7 do not affect images, the number of days between overpasses becomes 8. Both satellites provide images at a spatial resolution of  $30 \times 30$  m in the visible and near infrared portions of the electromagnetic spectrum. The thermal infrared band for Landsat 5 has a spatial resolution of  $120 \text{ m} \times 120 \text{ m}$  while Landsat 7 has a spatial resolution of  $60 \text{ m} \times 60 \text{ m}$ .

### **Description of procedure**

This chapter focuses on developing a sub-model for SEBAL that incorporates effects of advection. The model was developed under standard conditions and the criteria for standard conditions were alfalfa of height 40-60 cm, completely covering the ground, and not short of water. The rationale behind developing the sub-model under standard conditions first, then later transferring it to non-standard conditions, is based on the fact that the amount of advected horizontal heat energy that is converted to latent heat depends on surface conditions.

Advection as defined in this research is the horizontal transport of heat resulting from surface inhomogeneity (Zermono-Gonzalez and Hipps, 1997). However, not all the heat in the atmosphere just above the canopy is extracted. The amount of heat extracted from the atmosphere depends on surface roughness (Gay and Bernhofer, 1991), and how much of the extracted sensible heat is converted to latent heat depends on surface moisture conditions, with more sensible heat converted to latent heat when the surface is moist or when there is plenty of water in the soil available to vegetation. The proportion of the advected heat energy that is converted to latent heat therefore depends on the surface conditions, and is termed “effective advection” in this chapter and subsequent chapters.

## **Steps involved in the development of the advection sub-model**

### ***Selection of standard days***

Processed Landsat 5 and 7 images from 2010-2012, when either or both of the study fields satisfied the standard conditions, were selected. Those images were selected for model development. A crop log that included crop height was used to select the days when the alfalfa was 40-60 cm tall. The SEBAL-based EF was then used to determine whether or not the alfalfa was water-stressed, and fields with  $EF > 0.96$  were selected as satisfying the standard conditions. Fourteen images, as listed in Table 2.1 satisfied both criteria and therefore used.

### ***Model Development dataset***

For model development, available data were split into training (model development) and testing (validation) datasets. To have enough data for both training and testing processes, non-overpass days were used as training dataset, then overpass days as testing dataset. For the training dataset, 5 days prior to each of the satellite overpass days were used. This assumed that these 5 days had the same standard conditions as the day of overpass. This assumption was valid unless within the 5 days there was irrigation or rainfall, in which case the day and the days prior to irrigation or rainfall event would be discarded. Twenty-seven days were used in the development of the sub-model.

### ***Parameterization of advection under standard surface conditions***

A semi-empirical approach based on the concept of advective enhancement on evaporation as suggested by McNaughton (1976) was used. The concept states that evaporation

(E) can be expressed as the sum of equilibrium evaporation ( $E_{eq}$ ) due to available energy at the site, and enhanced evaporation ( $E_{ad}$ ) due to extra energy brought in by advection.

$$E = E_{eq} + E_{ad} \quad (2.1)$$

Hobbins et al. (2001) illustrates Penman's expression of potential ET as shown in Equation 2.2 which gives a similar concept of advective enhancement:

$$\lambda ET_p = \frac{\Delta}{\Delta + \gamma} Q_n + \lambda \frac{\gamma}{\Delta + \gamma} E_a \quad (2.2)$$

where  $\lambda$  is the latent heat of vaporization ( $J\ kg^{-1}$ ),  $\gamma$  is the psychrometric constant,  $\Delta$  is the slope of the temperature-saturation vapor pressure relationship ( $kPa\ ^\circ C^{-1}$ ),  $Q_n$  is the available energy and  $E_a$  is the drying power of the atmosphere. The first term is the equilibrium ET, which is ET resulting from available energy at the surface ( $R_n - G$ ). The second term represents ET resulting from advection, which Tolk et al. (2006) refer to as 'imposed ET' ( $ET_{imp}$ ).

Priestly and Taylor (1972) gave the first term of Equation 2.2 as:

$$\lambda ET_w = \alpha \frac{\Delta}{\Delta + \gamma} Q_n \quad (2.3)$$

where  $\lambda ET_w$  is the ET from a wet surface, at partial equilibrium, acknowledging that it is rare to have non-advective conditions, and  $\alpha$  is the Priestly-Taylor coefficient. Priestly and Taylor (1972) gave the value of  $\alpha$  as 1.26. However, various researchers have found different values of  $\alpha$ , ranging from 1.05 to 1.33 (Davies and Allen, 1973; McNaughton and Black, 1973). DeBruin and Keijman (1979) observed that  $\alpha$  has a diurnal and seasonal variation.

The uncertainties surrounding the value of  $\alpha$ , make the estimation of ET at partial equilibrium difficult. In SEBAL, the latent heat flux for a specific pixel is determined using the available energy ( $R_n - G$ ), and when water is non-limiting, the available energy equals the latent heat over vegetated surfaces. Therefore, if standard conditions, as earlier described, are assumed, the net radiation for the day will all be used for evaporation. Therefore, net radiation will equal

equilibrium latent heat, and Equation 2.2 can be re-written to be as shown in Equation 2.4. The soil heat flux,  $G$ , is thought to be close to zero on vegetated surfaces when averaged over the day, and therefore not included.

$$\lambda ET_{24} = R_{n24} + \lambda E_{ad24} \quad (2.4)$$

The advective component can be represented in the form shown in Equation 2.5:

$$\lambda ET_{ad24} = \frac{\gamma}{\Delta + \gamma} E_a \quad (2.5)$$

In most cases  $E_a$ , which is the drying power of the atmosphere, is calculated as a function of horizontal wind speed measured at a certain height (e.g., 2 m) and the vapor pressure deficit (Hobbins et al., 2001), with the common approach being:

$$E_a = f(u) \times (e_s - e_a) \quad (2.6)$$

where  $e_s$  and  $e_a$  are saturation and actual vapor pressures, respectively, and  $f(u)$  is the wind function. Different approaches have been suggested for the wind function, with Penman (1948) giving an empirical linear approximation:

$$f(u) = a(1 + bu_2) \quad (2.7)$$

where the values of ‘a’ and ‘b’ are 0.0026 and 0.54 respectively, and  $u_2$  is daily average wind speed at 2 m height given in  $m\ s^{-1}$ , and  $E_a$  in  $mm\ d^{-1}$ . However, the values of coefficients ‘a’ and ‘b’ are influenced by surface roughness and stomatal conductance, which then necessitates parameterization for specific surfaces. Brutsaert and Stricker (1979) suggested a theoretical approach rather than empirical where:

$$f(u) = \frac{\varepsilon a_v k^2 u_r}{R_d T_a \ln\left[\frac{z_2 - d_0}{z_{ov}}\right] \ln\left[\frac{z_r - d_0}{z_{om}}\right]} \quad (2.8)$$

where  $\varepsilon$  is the ratio of the gas constant of dry air,  $R_d$ , to that of water vapor,  $R_v$ ;  $a_v$  is the ratio of the eddy diffusivity to the eddy viscosity under neutral conditions;  $k$  is the von Karman constant,  $z_{om}$  and  $z_{ov}$  are the roughness lengths for momentum and water vapor, respectively;  $T_a$  is the air

temperature in Kelvin;  $z_2$  is the height (m) at which  $e_a$  is measured;  $d_o$  is the zero plane displacement height (m); and  $z_r$  is the height of the wind measurement (m).

Wright (1996) developed a wind function for alfalfa in southern Idaho expressing it as a linear function of mean wind speed:

$$f(u) = aw + (bw)U \quad (2.9)$$

where  $U$  is the wind speed, and ‘aw’ and ‘bw’ are empirically derived coefficients, and the coefficients depend on aerodynamic characteristics of the surface and the climatic characteristics of the region. He developed exponential equations for ‘aw’ and ‘bw’ for the wind function as:

$$aw = 0.4 + 1.4 \exp\left(-\left(\frac{D-173}{58}\right)^2\right) \quad (2.10)$$

$$bw = 0.605 + 0.345 \exp\left(-\left(\frac{D-243}{80}\right)^2\right) \quad (2.11)$$

where  $D$  is the calendar day of year (DOY). He explained that ‘aw’ seem to change as the day length changes, and ‘bw’ accounts for changes in dryness of regions surrounding the irrigated lands. This explains the inclusion of the DOY, but also makes Equations 2.10 and 2.11 local-specific.

Stigter (1980) suggested an equation, which shares some similarities with Equation 2.8 as it incorporates an aerodynamic parameter in the wind function:

$$f(u) = \frac{8(1+\frac{u}{100})}{[\ln\frac{(z_2-d)}{z_{om}}]^2} \quad (2.12)$$

where  $z_2$  is the height of measurement,  $d$  is the zero-plane displacement height and  $z_{om}$  is the roughness length for momentum. Both  $d$  and  $z_{om}$  can be estimated based on the height of the standing crop ( $h$ ), with  $d$  estimated to be  $0.67h$  and  $z_{om}$  to be  $0.123h$ . For regional estimation of ET, measuring the crop height represented in each pixel would be impossible. In SEBAL,  $z_{om}$  is

determined by using satellite-based NDVI values for each pixel, and the relationship is shown in Equation 2.13.

$$z_{om} = \exp(a \times NDVI + b) \quad (2.13)$$

where ‘a’ and ‘b’ are constants empirically obtained by relating satellite-obtained NDVI from a sample of pixels in the image to measured heights of vegetation in the area corresponding to the sampled pixels. The values of ‘a’ and ‘b’ are local specific and depend on the vegetation. Variation of the constants may be less with similar vegetation (e.g., agricultural as opposed to forests). A modified version of Equation 2.12 was used in this study to estimate the wind function, and the modification is explained later in the chapter.

When  $E_a$  and consequently  $\lambda E_{ad}$  had been determined, the latter was then introduced into the  $ET_{24}$  sub-model of SEBAL, which was modified from the original form of:

$$ET_{24} = \frac{86,400 \times EF \times Rn_{24}}{\lambda \times \rho_w} \quad (2.14)$$

to the form with the advective component:

$$ET_{24} = \frac{86,400 \times EF \times (Rn_{24} + \lambda E_{ad})}{\lambda \times \rho_w} \quad (2.15)$$

It should be noted that under standard conditions, EF is close to 1; therefore ET is equivalent to the total energy available, which is the sum of net radiation and advected energy.

### ***Modified SEBAL model validation***

The developed model was then applied to the 14 images that satisfied the standard conditions. This was done by using the afternoon wind run and daily average VPD and maximum and minimum temperatures to model effective advection for each of the satellite overpass days. Subsequently, the effective advected energy was introduced into SEBAL

algorithm as shown in Equation 2.15, to obtain a new daily ET value that incorporated the advection effects on the evaporation process (on a daily time-step).

### ***Modified SEBAL model evaluation***

The alfalfa daily ET estimated using the modified SEBAL was then compared to alfalfa daily ET measured using the lysimeters. The statistical indicators used to evaluate the model performance were: coefficient of determination ( $R^2$ ), mean bias error (MBE), root mean square error (RMSE) and the Nash-Sutcliffe coefficient of efficiency (NSCE). These indicators were defined in Chapter 1. The performance of modified SEBAL was also compared to that of the original SEBAL to evaluate if there was any improvement.

### **Requirement of wind data in SEBAL**

#### ***At time of satellite overpass***

Wind speed and in some cases solar radiation measurements is the only ground data required for SEBAL. The wind speed should be measured at the time of satellite overpass as it is used in the calculation of sensible heat flux (H). However in some areas, the wind speed at the exact time of overpass may not be available, as only the daily wind run is recorded.

Several approaches may be used to estimate instantaneous wind speed from daily wind runs or daily maximum and minimum wind speed. One approach is to model the diurnal variation of wind speed (Peterson and Parton, 1983; Zhang and Zheng, 2004; Ephrath et al., 1996), often using the relationship between wind speed and surface air temperature and/or vapor pressure deficit. Peterson and Parton (1983) found that it is possible to simulate the diurnal variation of surface wind speed using the air temperature variation. Since the diurnal variation of

air temperature can be estimated more accurately using the maximum and minimum temperatures as explained in Campbell and Norman (1998), the temperature diurnal pattern obtained can be used to model wind speed for any particular time of day. The inputs for the model to estimate wind speed include day length, and maximum and minimum daily wind speeds, and is given by the equations:

$$S_d = (SMX - SMN) \times \sin \left[ \frac{\pi \times BBM}{ADY + 2a} \right] + SMN \quad (2.16)$$

$$S_n = (SSN - SMN) \times \exp \left[ \frac{-b \times BBN}{ANI} \right] + SMN \quad (2.17)$$

where  $S_d$  is wind speed during the day,  $S_n$  is wind speed during the night in  $m s^{-1}$ ,  $SMX$  and  $SMN$  are maximum and minimum wind speeds ( $m s^{-1}$ ),  $SSN$  is the wind speed at sunset,  $ADY$  and  $ANI$  are day and night length in hours,  $BBM$  is the number of hours from the hour of minimum wind speed to sunset,  $BBN$  is the number of hours from sunset to the hour of minimum wind speed.

In another method, Ephrath et al. (1996) observed that wind speed is low in the early hours of morning, then it increases up to late afternoon, and then decreases to a minimum value in the evening. From these observations, they developed a model that required total wind run, periods in which wind speed increases from the minimum value and decreases back to this value, and also using the value of maximum wind speed. The wind speed at a given time is therefore estimated as follows:

$$W_a = W_{min} + W_{max} \times \sin \left( 2 \times \pi \times \frac{t_a - tw_{1,2}}{SF_{1,2}} \right) \quad (2.18)$$

where  $W_a$  is the wind speed ( $m s^{-1}$ ) at a certain time,  $W_{min}$  is the minimum wind speed,  $W_{max}$  is the maximum wind speed,  $tw_{1,2}$  and  $SF_{1,2}$  are time interval factors, which are empirically obtained.

From the description of the methods above, it can be noted that modeling wind speed requires many inputs, which may still be unavailable when one only has the daily wind run. Therefore if the wind speed at time of overpass is not available, an alternative would be to use either the daily average which can be calculated from the daily wind run, or as suggested in FAO 56 (Allen et al., 1998), a value of  $2 \text{ m s}^{-1}$  can be used for missing wind speed data. The  $2 \text{ m s}^{-1}$  was found by Allen et al. (1998) to be the average wind speed measured in over 2000 weather stations worldwide.

To determine how wind speed would affect the accuracy of ET when using SEBAL, a sensitivity analysis was carried out. Six days of satellite overpass were used and 3 levels of wind speed used for each day; light wind ( $1.0 \text{ m s}^{-1}$ ), moderate wind ( $2 \text{ m s}^{-1}$ ) and strong wind ( $5 \text{ m s}^{-1}$ ).

From the results shown in Table 2.2, it can be concluded that the SEBAL model is relatively less sensitive to wind speed in estimating ET, as the maximum error would be about 5 %, and in most cases, it would not exceed 2 %. This therefore means using either the daily average wind speed or  $2 \text{ m s}^{-1}$  would not significantly affect the accuracy of ET estimation.

### ***Afternoon wind run for advection modeling***

In Chapter 1, it was noted that the afternoon wind represents advection better than the 24-hr wind run as advection mostly takes place in the afternoon when there are higher wind speeds, and at that time the air is usually warm and dry. Therefore in the advection sub-model, the afternoon wind run was used instead of the 24-hr. However, when there are no automatic recordings of wind speed in the afternoon, modeling of wind speed becomes necessary. An

alternative to that would be to record the wind, more than once on the day of satellite overpass. At least three recordings through the day would be required; at sunrise, midday and sunset.

## RESULTS AND DISCUSSIONS

### Parameterization of advection under standard conditions

For this research, a modification was made on Stigter (1979) equation, which is Equation 2.12. The modification process was carried out using the training data, and the steps are outlined in Appendix A4. The resulting equation was:

$$f(u) = \frac{8\left(\frac{T_{max}}{20}\right)\left(\frac{T_{min}}{10}\right)\left(1 + \frac{U}{100}\right)}{\left[\ln\left(\frac{z_2-d}{z_{om}}\right)\right]^2} \quad (2.19)$$

Where  $T_{max}$  and  $T_{min}$  are the day's maximum and minimum temperatures respectively and  $U$  is the wind run ( $\text{km d}^{-1}$ ). The modification in Equation 2.19 includes a temperature parameter. The drying power of air ( $E_a$ ) is a combination of vapor pressure deficit (VPD) and the wind function, as illustrated in Equation 2.6. The VPD represents the capacity of air to accept vapor from the evaporation surface, and while temperature may influence VPD, it also determines the amount of heat energy that is brought onto the evaporating surface, thus a wind function with both wind and temperature variables has more physical meaning.

The day's extreme temperatures, rather than the mean temperature are used in Equation 2.19, and they give a more accurate estimate of advection. The maximum temperature gives an estimate of the heat content of the air brought onto the evaporating surface on the advective afternoons. The minimum temperature on the other hand gives an indication of the possibility of having evening/night ET. In Chapter 1, it was observed that some evapotranspiration, though not much (because of decreased stomatal conductance), does take place in the absence of solar

radiation on advective days. As high as 2 mm of ET, was observed as shown in Chapter 1, Table 1.4, on 22 May 2010. Including the minimum temperature distinguishes conditions where the temperature might be high enough for evening ET to take place. The 20 °C and 10 °C denominators in Equation 2.19 were obtained by trial and error. It must be noted that in cases where the minimum temperature was below 10 °C, a minimum of 10 °C was used, so as to make the fraction unity.

Equation 2.19, similar to Equation 2.12, accounts for the aerodynamic characteristics, which is influenced by surface roughness conditions. Although the equation was developed on standard conditions, it was expected that it would be transferable to surfaces of different roughness because of the roughness component. However, stomatal resistance and fraction of vegetation cover were not factored in the equation, with the assumption that the EF as used in Equation 2.15 would account for those.

Upon development of the final version of the wind function as it is in Equation 2.19, the advection model was found to sufficiently estimate the advection component. When using the training data to develop the advection model, and therefore modifying the SEBAL model, the resulting performance of the modified SEBAL model when compared with lysimeter ET was an MBE of  $-0.08 \text{ mm d}^{-1}$  (-1.3 %), and RMSE of  $0.67 \text{ mm d}^{-1}$  (10.9 %) and the NSCE was 0.77 (Figure 2.2).

### **Modified SEBAL testing**

After the model was developed, it was tested using Landsat 5 and 7 images for overpass days. Using Equation 2.19 to determine the wind function, the drying power ( $E_a$ ) and the

advected energy ( $E_{ad}$ ) were then determined. Then  $E_{ad}$  was included in the  $ET_{24}$  sub-model, as given in Equation 2.15.

Table 2.3 shows the results of the modification, and compares the errors in the modified SEBAL model with the original SEBAL. On average, the original SEBAL underestimated Alfalfa ET by 17 %, with underestimations of up to 38 %, while the modified SEBAL had an average overestimation of about 2.2 %, with all errors within 20 % except one on 5 August 2010 which had an ET error of 24 %. Table 2.3 shows statistics for both the original and modified SEBAL, with the latter showing significant improvement over the original SEBAL. The Mean Bias Error of  $-1.3 \text{ mm d}^{-1}$  (-17.1 %) in the original SEBAL was reduced to  $0.17 \text{ mm d}^{-1}$  (2.2 %) with modified SEBAL, and Root Mean Square Error reduced from  $1.9 \text{ mm d}^{-1}$  (25.1 %) to  $0.83 \text{ mm d}^{-1}$  (10.9 %). An original NSCE of -0.03, which suggested that the SEBAL model was unsuitable to estimate daily ET, was improved to a good value of 0.81 with modified SEBAL.

Figures 2.3 and 2.4 show graphs of ET determined using the original and modified SEBAL respectively, drawn versus lysimeter-measured alfalfa ET. Modified SEBAL compares very well with the lysimeter, whilst the original SEBAL underestimates ET. The underestimation was largest for higher ET values, possibly where there was more advection. For the modified SEBAL, most of the points were close to the 1:1 line.

Figure 2.5 shows the results of the estimation of ET from the modified SEBAL when the 24-hr wind was used instead of the afternoon wind. There was more underestimation observed on some days, when the 24-hour wind did not represent the period of advection.

It was also observed that the modified model did not improve the performance on non-advective days. However, on days when there was advection, there was a significant reduction in ET error. An example would be 19 September 2010 in field A, where the wind speed was

2.7 m s<sup>-1</sup>, RH was 56.7 % and the mean temperature was 22 °C, the error was reduced from an absolute error of 29.9 % to 8.9 % (Table 2.4). The same was observed on 22 May 2010 in field A when the wind speed was 3.8 m s<sup>-1</sup>, RH was 28.0 % and the mean temperature was 23.2 °C, and the error was reduced from 35.6 % to 6.5 %. The ability of the modified SEBAL model to reduce the MBE to close to zero is an important quality as it gets rid of the bias, and that would help as the seasonal ET would be more accurately estimated as opposed to gross underestimation with the original SEBAL, which consistently underestimates ET.

## CONCLUSION

The ET<sub>24</sub> sub-model for SEBAL was modified by including modeled advection. The approach significantly improved the performance of SEBAL under advective conditions. These conditions are a common occurrence in arid and semi-arid regions. The development of this model improves SEBAL estimates of ET in regions where there is advection, and where weather data are not sufficient to use METRIC. The MBE for the modified SEBAL was 0.17 mm d<sup>-1</sup> (2.2 %) compared to -1.3 mm d<sup>-1</sup> (-17.1 %) for original SEBAL, RMSE was reduced from 1.9 mm d<sup>-1</sup> (25.1 %) to 0.83 mm d<sup>-1</sup> (10.9 %), and the NSCE for the modified SEBAL was 0.81 which is considered good, compared to -0.03 for original SEBAL which indicate the model is not appropriate.

The model involved the development of the wind function, estimation of the amount of advected energy and then summing net radiation and advective energy in the ET<sub>24</sub> sub-model. The resulting ET is therefore the sum of ET due to vertical radiant energy and enhanced ET due to horizontal advection of sensible heat. The development and also application of the advection model requires maximum and minimum temperatures, RH and wind run.

It was observed that when afternoon wind run was used in the wind function, SEBAL estimated more accurately the alfalfa ET than when the 24-hour wind run was used. This occurred because the afternoon winds represented advective conditions better as advection occurs mostly in the afternoon when it is windy, and when the air is warmer and drier. The model is expected to perform fairly well in different surfaces as it has an aerodynamic function, even though it was developed under standard conditions (i.e., for a healthy vigorously growing alfalfa, 40-60 cm tall canopy and not short of water).

## **RECOMMENDATIONS**

- a. Since the use of afternoon wind run seemed to give more accurate estimation of ET than when 24-hour wind run is used, it is recommended that it be used in the modeling of advection. However, where there are no automated wind speed sensors and only a 24-hour wind run is available, it is recommended that on days of satellite overpass, at least 3 visits be made to record the wind run; in the morning, at noon, and at sunset. This ensures that the wind run used represents the period when there is advection.
- b. The model should be tested for non-standard conditions to determine if the model could be applicable across a range of crops, and how water stress would affect the results.

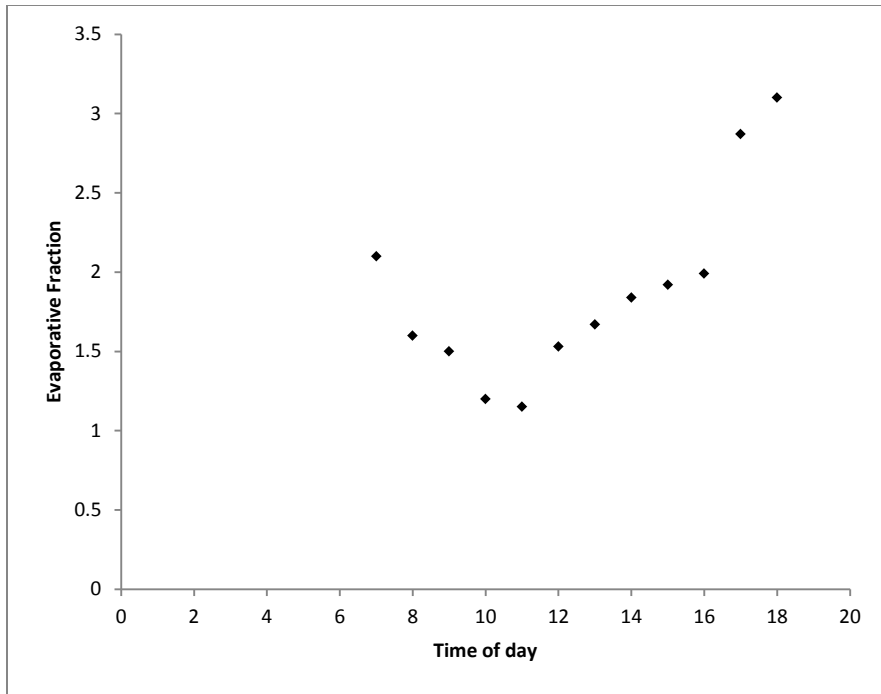


Figure 2.1: Diurnal variation of evaporative fraction on 22 July 2010 at Rocky Ford, CO showing effects of advective conditions

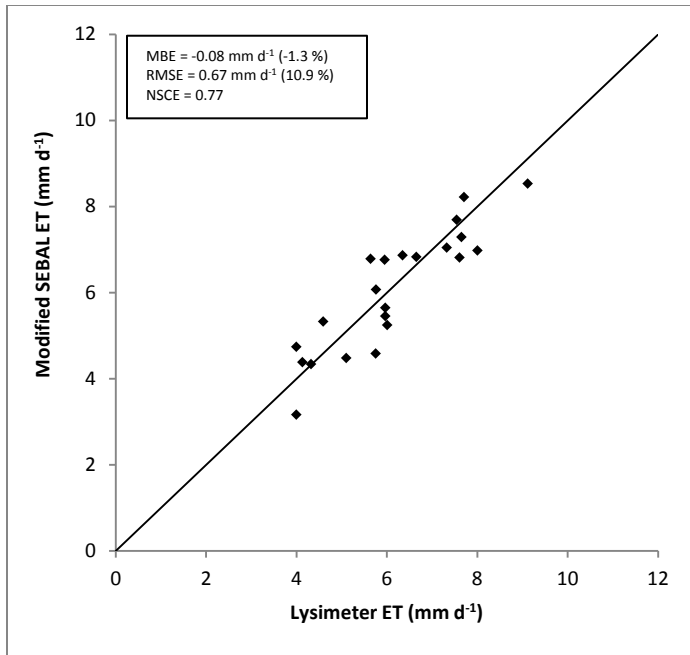


Figure 2.2: Comparing modified SEBAL-modeled and Lysimeter-measured daily alfalfa ET using the training data

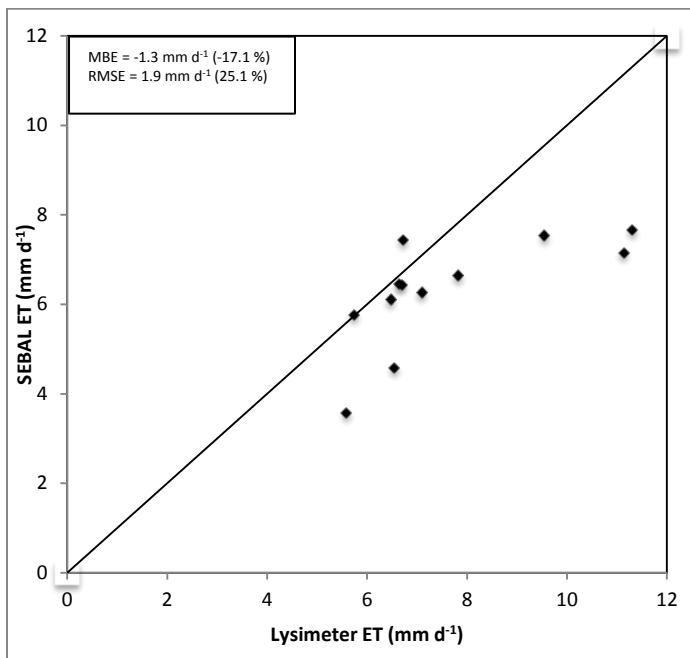


Figure 2.3: Comparing SEBAL-modeled and Lysimeter-measured daily alfalfa ET under standard conditions

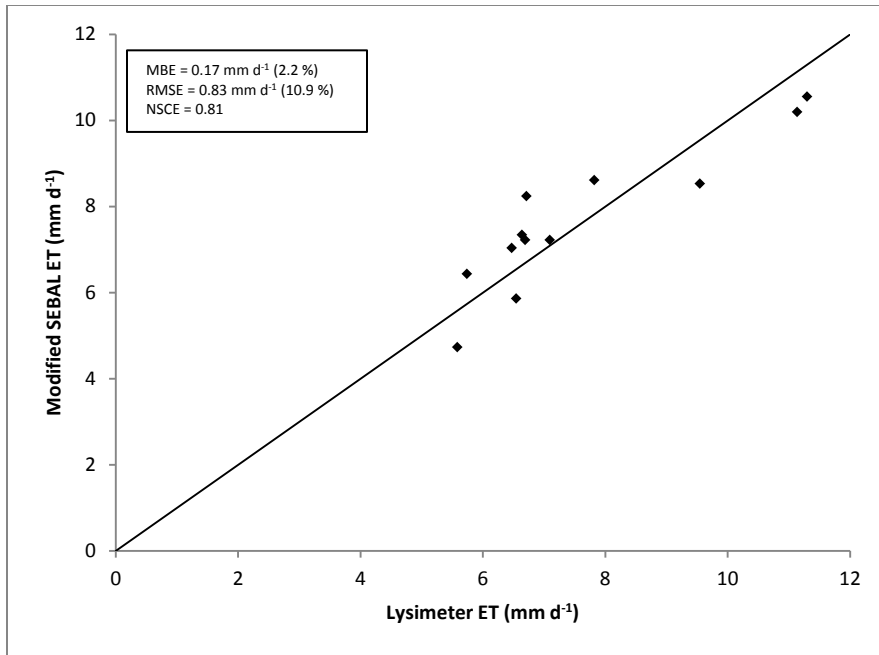


Figure 2.4: Comparing modified SEBAL and Lysimeter-measured daily alfalfa ET under standard conditions

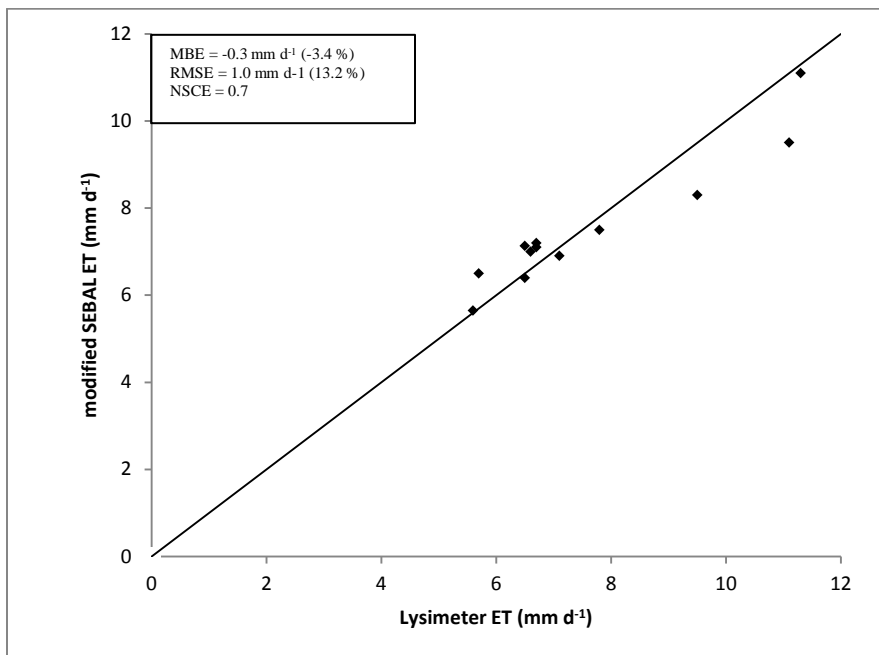


Figure 2.5: Comparison of modified SEBAL-modeled and lysimeter-measured daily alfalfa ET when the 24-hr wind run is used instead of afternoon wind run.

Table 2.1: Standard days with alfalfa height and evaporative fraction

<b>Date</b>	<b>Crop height (cm)</b>	<b>EF</b>
06 May 2010	43	0.972
22 May 2010	60	0.987
22 May 2010	48	0.984
10 Aug 2010	50	0.993
18 Aug 2010	55	0.997
19 Sep 2010	46	0.985
05 Oct 2010	55	0.982
05 Aug 2011	55	1.002
04 Jul 2011	57	0.999
05 Aug 2011	56	0.991
21 Aug 2011	60	0.998
21 Aug 2011	59	0.986
20 Jun 2012	43	0.988
22 Jul 2012	53	0.992

Table 2.2: Alfalfa ET estimation using SEBAL for three levels of wind speed

<b>Date</b>	<b>SEBAL ET (mm/d)</b>		
	<b>1 m/s</b>	<b>2 m/s</b>	<b>5 m/s</b>
22 May 2010	6.76 (0.5 %)*	6.72	6.41 (-4.6 %)
15 June 2010	6.89 (2.1 %)	6.74	6.51 (-3.4 %)
10 Aug 2010	6.36 (2.9 %)	6.18	6.15 (-0.6 %)
26 Aug 2010	3.42 (1.46 %)	3.37	3.37 (0 %)
11 Sept 2010	4.70 (2.0 %)	4.61	4.61 (0 %)
27 Sept 2010	4.15 (3.9 %)	4.00	3.62 (-2.3 %)

Table 2.3: Performance of models on overpass days, and calculated statistics

<b>DATE</b>	<b>LYSIMETER ET mm d<sup>-1</sup></b>	<b>SEBAL ET mm d<sup>-1</sup></b>	<b>SEBAL ERROR %</b>	<b><sup>1</sup>M-SEBAL ET mm d<sup>-1</sup></b>	<b>M- SEBAL <sup>2</sup>ERROR %</b>
08/18/10 (A)	6.6	6.5	-2.7	7.4	12.2
09/19/10 (A)	6.5	4.6	-29.9	6.0	-8.9
10/05/10 (A)	5.6	3.6	-38.9	4.8	-13.6
08/05/11(A)	6.7	7.5	10.9	8.3	24.1
05/06/10 (A)	7.8	6.7	-15.0	8.7	11.8
05/22/10 (A)	11.1	7.2	-35.6	10.4	-6.5
08/10/10 (A)	5.7	5.8	0.6	6.5	13.5
08/05/11(B)	6.7	6.4	-3.7	7.3	9.4
07/04/11(A)	9.5	7.5	-21.0	8.6	-9.5
08/21/11(A)	7.1	6.3	-11.7	7.3	3.3
06/20/12 (A)	11.3	7.7	-32.2	10.8	-4.7
08/21/11(B)	6.5	6.1	-5.6	7.1	10.3
<b>Statistics</b>					
MBE		-1.3	-17.1	0.17	2.2
RMSE		1.9	25.1	0.83	10.9
NSCE		-0.03		0.81	

<sup>1</sup>M-SEBAL is modified SEBAL

<sup>2</sup>Error is the discrepancy between lysimeter measured ET and the model estimated ET, with positive error being overestimation and negative error being underestimation of ET by model when compared to the lysimeter

Table 2.4: Satellite overpass days with weather details and errors for both SEBAL versions

DATE	LYSIMETER				SEBAL	*SEBAL	M-SEBAL ET	M-SEBAL
	ET mm	T <sub>a</sub> °C	RH %	U m s <sup>-1</sup>	ET Mm	ERROR %		ERROR %
81810 (A)	6.6	24.3	55.5	0.8	6.5	-2.7	7.4	12.2
91910 (A)	6.5	22.0	56.7	2.7	4.6	-29.9	6.0	-8.9
100510(A)	5.6	18.7	57.1	1.7	3.6	-38.1	4.8	-13.6
080511(A)	6.7	23.8	63.9	0.9	7.5	10.9	8.3	24.1
50610 (A)	7.8	16.0	41.0	4.3	6.7	-15.0	8.7	11.8
52210 (A)	11.1	23.2	28.0	3.8	7.2	-35.6	10.4	-6.5
81010 (A)	5.7	23.0	69.1	0.9	5.8	0.6	6.5	13.5
080511(B)	6.7	23.9	64.3	0.9	6.4	-3.7	7.3	9.4
70411 (A)	9.5	24.4	49.8	1.1	7.5	-21.0	8.6	-9.5
082111(A)	7.1	23.7	62.9	1.2	6.3	-11.7	7.3	3.3
062012(A)	11.3	23.1	43.6	3.4	7.7	-32.2	10.8	-4.7
082111(A)	6.5	23.6	64.0	1.2	6.1	-5.6	7.1	10.3

\*Error is the discrepancy between lysimeter measured ET and the model estimated ET, with positive error being overestimation and negative error being underestimation of ET by model when compared to the lysimeter

## REFERENCES

Allen RG, Pereira LS, Raes D, Smith M (1998) Crop evapotranspiration – guidelines for computing crop water requirements. FAO Irrigation and drainage paper 56. Food and Agriculture Organization of the United Nations. Rome.

Allen RG, Tasumi M and Morse A (2005) Satellite-based evapotranspiration by energy balance for western states water management. US Bureau of Reclamation Evapotranspiration Workshop. February 8-10, 2005.

Bastiaanssen WGM, Noordman EJM, Pelgrum H, Davids G, Thoreson BP, Allen RG (2005) SEBAL Model with remotely sensed data to improve water resources management under actual field conditions. *Journal of Irrigation and Drainage Engineering*, 131 (1):85-93.

Brutsaert W and Stricker H (1979) An advection-aridity approach to estimate actual regional evapotranspiration. *Water Resour. Res.* 15(2): 443-450.

Brutsaert W and Sugita M (1992) Application of self-preservation in the diurnal evolution of the surface energy budget to determine daily evaporation. *J. Geophys. Res.* 97, 18:377-18, 382.

Campbell GS and Norman JM (1998) An introduction to environmental biophysics. Second edition. Springer. NY, USA.

Crago RD and Brutsaert W (1996) Daytime evaporation and the self-preservation of the evaporative fraction and the Bowen ratio. *J. Hydrol.*, 178, 241-255.

Davies JA and Allen CD (1973) Equilibrium, potential and actual evaporation from cropped surfaces in southern Ontario. *J. Appl. Meteorol.* 12: 649-657.

DeBruin HAR and Keijman JQ (1979) Priestly-Taylor evaporation model applied to a large, shallow lake in the Netherlands. *J. Appl. Meteorol.* 18(7): 898-903.

Ephrath JE, Goudriaan J, Marani A (1996) Modelling diurnal patterns of air temperature, radiation, wind speed and relative humidity by equations from daily characteristics. *Agricultural Systems.* 51(4): 377-393.

Farah HO, Bastiaanssen WGM, Feddes RA (2004) Evaluation of the temporal variability of the evaporative fraction in a tropical watershed. *International Journal of Applied Earth Observation and Geoinformation.* 5: 129-140.

Gay LW and Bernhofer C (1991) Enhancement of evaporation by advection in arid regions: Hydrological interactions between atmosphere, soil and vegetation. Proceedings of the Vienna Symposium, August 1991. IAHS Publ. no. 204.

Gentine P, Entekhabi D, Polcher J (2011) The Diurnal Behaviour of Evaporative Fraction in the Soil-Vegetation-Atmospheric Boundary Layer Continuum. *Journal of Hydrometeorology.*

Hobbins MT, Ramirez JA, Brown TC (2001) The complementary relationship in estimation of regional evapotranspiration: An enhanced Advection-Aridity model. *Water Resources Research*, Vol. 37(5): 1389-1403.

Hoedjes JCB, Chehbouni A, Jacob F, Ezzahar J, Boulet G (2008) Deriving daily evapotranspiration from remotely sensed instantaneous evaporative fraction over olive orchard in semi-arid Morocco. *Journal of Hydrology*, 354: 53-64.

Lhomme JP and Elguero E (1999) Examination of evaporative fraction diurnal behavior using a soil-vegetation model coupled with a mixed-layer model. *Hydrology and Earth System Sciences*, 3(2):259-270.

McNaughton KG (1976) Evaporation and advection I: evaporation from extensive homogenous surfaces. *Quart. J. R. Met. Soc.* 102: 181-191.

McNaughton KG and Black TA (1973) Study of evapotranspiration from a Douglas-fir forest using energy-balance approach. *Water Resour. Res.* 9(6): 1579-1590.

Nichols WE and Cuenca RH (1993) Evaluation of the evaporative fraction for parameterization of the surface energy balance. *Wat. Resour. Res.*, 29, 3681-3690.

Penman HL (1948) Natural evaporation from open water, bare soil and grass. *Proc. R. Soc. London, Ser. A*, 193, 120-146.

Peterson TC and Parton WJ (1983) Diurnal variations of wind speeds at a short grass prairie site – A model. *Agricultural Meteorology*. 28: 365-374.

Priestly CHB and Taylor RJ (1972) On the Assessment of Surface Heat Flux and Evaporation Using Large-Scale Parameters. *Mon. Weather Rev.* 100:81-92.

Shuttleworth WJ, Gurney RJ, Hsu AY, Ormsby JP (1989) FIFE: the variation in energy partition at surface flux sites. *IAHS Publ.* 186: 67-74.

Singh RK, Irmak A, Irmak S, Martin DL (2008) Application of SEBAL Model for mapping evapotranspiration and estimating surface energy fluxes in South-Central Nebraska. *Journal of Irrigation and Drainage Engineering*, 134 (3): 273-285

Stewart JB (1996) Extrapolation of evaporation at time of satellite overpass to daily totals. In: J.B. Stewart et al. (editors) *Scaling up in Hydrology using Remote Sensing*. Wiley, Chichester, UK.

Stigter CJ (1980) Assessment of the quality of generalized wind functions in Penman's equations. *Journal of Hydrology*, 45: 321-331.

Suleiman AA, Bali KM, Kleissl J (2009) Comparison of ALARM and SEBAL Evapotranspiration of Irrigated Alfalfa. 2009 ASABE Annual International Meeting.

Tolk JA, Evett SR, Howell TA (2006) Advection Influences on Evaporation of Alfalfa in a Semiarid Climate. *Agron. J.* 98:1646-1654.

Wright JL (1996) Derivation of alfalfa and grass reference evapotranspiration. In. Evapotranspiration and Irrigation Scheduling. C.R. Camp, E.J. Sadler, and R.E. Yoder (ed.). Proc. Int. Conf., ASAE, San Antonio, TX. P. 133-140.

Zhang D and Zheng W (2004) Diurnal cycles of surface winds and temperatures as simulated by five boundary layer parameterizations. *Journal of Applied Meteorology.* 43: 157-169.

Zermeño-Gonzalez A and Hippias LE (1997) Downwind evolution of surface fluxes over a vegetated surface during local advection of heat and saturation deficit. *Journal of Hydrology* 192: 189-210.

## CHAPTER 3

### Evaluating the transferability of the modified SEBAL model

#### Overview

The Surface Energy Balance Algorithm (SEBAL) was modified by incorporating an advection component as part of the energy usable for evapotranspiration. This was to correct for the tendency of the SEBAL model to underestimate ET under conditions of advection. A model used to estimate the advected energy required the development of a wind function. In Chapter 2, the modified SEBAL model was developed and tested on alfalfa of a standard height, which was not short of water. The objective of this section of the research was to test the developed model on different crops and conditions to evaluate its transferability. The crops used for the test were beans, wheat and corn. The estimated ET using the modified SEBAL model was compared to actual ET measured using the Bowen Ratio Energy Balance (BREB) system. The modified SEBAL model estimated ET fairly well on beans and wheat, only showing some slight underestimation, with an MBE of  $-0.7 \text{ mm d}^{-1}$  (-11.3 %) and RMSE of  $0.82 \text{ mm d}^{-1}$  (13.9 %) and an NSCE of 0.64. When the modified SEBAL model was tested on fully irrigated corn, it performed well, resulting in no bias, i.e. an MBE of  $0.0 \text{ mm d}^{-1}$  and RMSE of  $0.78 \text{ mm d}^{-1}$  (10.7 %) and NSCE of 0.82. The model seemed to incur some errors on corn, which was either water-stressed, or at early stages of growth. It was concluded that the modified SEBAL could be used on a wide range of crops if they are adequately irrigated, therefore not short of water. It was recommended that the model be further adjusted so that it can accurately estimate ET under dry conditions.

## INTRODUCTION

In the previous chapter, a modification was made on SEBAL by introducing an advection component into the 24-h evapotranspiration ( $ET_{24}$ ) sub-model of the SEBAL ET algorithm. The original SEBAL model did not account for advection resulting in ET underestimation on advective days, so it was modified to include advection. Daily averages of vapor pressure deficit (VPD), wind speed ( $u$ ), relative humidity (RH) and air temperature ( $T_a$ ) were used in the parameterization of the advection correction in SEBAL. It was explained in the previous chapter that the model developed did not estimate advection per se, but rather the portion of advected energy that could be captured and converted to latent heat. That advected energy or portion was referred to as effective advection. Since effective advection depends on surface conditions, it was necessary to describe the conditions under which the model was developed, and these conditions are in this research referred to as standard conditions. The criteria for standard conditions were alfalfa within the height range of 40-60 cm, completely covering the ground, and not short of water. The absence of water stress was indicated by the instantaneous evaporative fraction ( $EF_{inst.}$ ) being approximately 1 ( $EF > 0.96$ ).

It was reasoned that a specific vegetated surface is able to capture a certain amount of advected sensible heat from the atmosphere, and then convert a portion of that horizontal sensible heat to latent heat. The converted portion of advection was termed “effective advection”. Advection in this research was defined as the horizontal transport of heat resulting from surface inhomogeneity (Zermono-Gonzalez and Hipps, 1997). Not all the advected heat in the atmosphere just above the canopy is extracted and how much of it is extracted depends on the surface roughness. When the sensible heat has been extracted, some of it is converted to latent

heat, depending on the surface moisture conditions, and the final amount converted to latent heat becomes the energy equivalent of advection-enhanced evapotranspiration.

Although the advection sub-model in Chapter 2 was developed under standard conditions, it included an aerodynamic parameter, which makes it account for differences in surface roughness. However, it was still necessary to test the model for transferability (i.e., evaluating it across various vegetated surface conditions) to different crop types, growth stages and soil moisture conditions. Then, if necessary further modify the model in order to produce a robust algorithm while still requiring as least amount of ground data as possible. In this chapter, the crop ET modeled using the modified SEBAL was compared to ET measured using a Bowen Ratio Energy Balance (BREB) system.

### **Surface roughness**

As previously explained, the portion of heat extracted from the atmosphere depends on surface roughness. Gay and Bernhofer (1991) mentioned that rough surfaces are more efficient in extracting sensible heat from the atmosphere. Surface roughness affects the aerodynamic mixing of water vapor and heat over a canopy.

Surface roughness is a function of several factors, some of them are: average height of roughness elements, their areal density, dynamic response characteristics, etc. (Arya, 2001). According to Campbell and Norman (1998), when we begin from a low plant density, as the density increases the roughness of the surface will also increase, up to a point where the increase in density will result in the surface being smoothed. Plant flexibility is also a factor in surface roughness; with rigid roughness elements (e.g., corn plants) more likely to result in larger surface

roughness than more flexible elements (e.g., alfalfa plants, which can bend in response to wind forces).

Surface roughness is mainly characterized by roughness length and displacement height (Arya, 2001; Prueger, 2004). The roughness length ( $z_o$ ), according to Prueger (2004) is related to the efficiency of exchange at the surface, but is not to be understood as a measurable physical length (Campbell and Norman, 1998). The zero-plane displacement height ( $d_o$ ) can be defined as the height at which momentum is absorbed within the roughness elements, these elements being plants when we refer to agricultural fields as the surfaces.

It is difficult to accurately estimate aerodynamic parameters (Matthias et al., 1990), and yet these parameters have a role in the estimation of sensible heat flux (H) and latent heat flux (LE) for remote sensing models that are based on the concept of energy balance, e.g. SEBAL. However, Allen et al. (2005) points out that the internal calibration of SEBAL and also METRIC reduces the impacts of inaccurate estimation of, among other parameters, surface roughness. Singh et al. (2008) agree that the value of  $z_o$  is not critical in the estimation of ET when using SEBAL.

However, when the roughness parameter is used in the estimation of advection that enhances ET, the accuracy of that parameter becomes consequential. According to research findings, roughness parameters can be estimated from measurable properties of the surface, for example the mean height of plants (Matthias et al., 1990; Campbell and Norman, 1998; Arya, 2001), with roughness length for momentum transport ( $z_{om}$ ) having been found to range between 0.10 and 0.15 of mean height and  $d_o$  at two-thirds of the height of homogeneous plant surfaces. Prueger (2004) pointed out that it is more difficult to estimate  $z_o$  and  $d_o$  when the surface has sparse vegetation, or for row crops at the early stages of growth. Hatfield (1989) indicated that

simply using a fraction of height to estimate  $z_0$  and  $d_0$  might be erroneous for surfaces that are partly covered. Campbell and Norman (1998) added that with row crops, the direction of the wind with respect to the rows might also affect the roughness length. In general, roughness length is expected to increase as the crop grows, and as density increases. However, completely closed canopies, which are very dense, are expected to have lower roughness than some level of sparse or row structured crops (Shuttleworth and Wallace, 1985) due to a phenomena Raupach (1994) referred to as “over-sheltering” where elements shelter one another and the air flow within canopy is separated from the air flow above the canopy.

In SEBAL, the surface roughness length for momentum transport is determined by using a calibrated model based on the normalized difference vegetation index (NDVI), a parameter defined in Chapter 1. The relationship is given as:

$$Z_{om} = \exp [a + (b \times NDVI)] \quad (3.1)$$

where ‘a’ and ‘b’ are constants that depend on local field conditions (Griske and Meijninger, 2005). These constants are obtained by relating NDVI and  $z_{om}$  for sample pixels that represent various vegetation types (Morse et al., 2000).

The fact that NDVI shows signs of saturation under high biomass conditions (Maskova et al., 2008) concurs with the tendency for roughness to increase with plant density up to a certain point whereby the surface is thereafter made smooth. This makes NDVI an appropriate index for roughness.

### **Surface moisture availability**

One of the criteria for standard conditions under which the advection parameterization process was carried out was that the vegetated surface (in this case alfalfa) or soil root zone

profile should not be short of water. The indicator used for such conditions was the instantaneous evaporative fraction ( $EF_{inst}$ ) of approximately 1, and the minimum used was 0.96, where  $EF_{inst}$  is the EF at the time of satellite overpass. The EF as previously defined is the ratio of latent heat to available energy, and an EF of 1 means all the energy available has been used for evapotranspiration; which is only likely to take place where water is readily available. In SEBAL, a pixel EF of less than 1 would indicate that evaporation is not at its maximum, either due to the field represented in the pixel having water-stressed plants or there being dry patches of soil exposed or both. Other explanations for  $EF < 1$  could be plant disease, lack of adequate nutrients available for the plant, high soil salinity, pest infestation, or lack of adequate gas exchange conditions in the root zone (e.g., waterlogging, compaction, etc.).

Since SEBAL regards net radiation as the only source of energy that can be used for ET and also assumes that EF is constant throughout the day, the model determines the daily ET as represented in Equation 3.2 below. The variables of the equation are defined in detail in Chapter 1, Equation 1.12.

$$ET_{24} = \frac{86,400 \times EF \times Rn_{24}}{\lambda \times \rho_w} \quad (3.2)$$

However, in the previous chapter, the equation was modified to include the advection component as shown in Equation 3.3.

$$ET_{24} = \frac{86,400 \times EF \times (Rn_{24} + \lambda E_{ad})}{\lambda \times \rho_w} \quad (3.3)$$

It makes sense to assume that when advected sensible heat interacts with a drier vegetated surface as in non-standard conditions, the effective advection will be less than what it would be if it were under standard conditions; in that case the advection component in the  $ET_{24}$  sub-model would need to be adjusted. The drier the surface, the likelihood is that the advected energy will not impact much on the ET, but instead will only enhance sensible heat flux.

Equation 3 assumes that the advection component can be adjusted using the same EF that is used for  $R_{n24}$ . However it should be noted that net radiation and advection have different ‘flow directions’, as net radiation can be assumed to be vertical while advection is horizontal, and therefore different angles of interaction with the surface. The result of the interaction of advected energy with the partly dry surfaces in row crops may also depend on wind direction in relation to the field row orientation, which adds complexity to the estimation of effective advection.

### Description of BREB method

In this chapter, the modified SEBAL-modeled ET was compared to ET measured using the Bowen ratio and energy balance (BREB) method. The BREB method, as the name suggests, is based on the energy balance, and uses the ratio of sensible heat flux to latent heat flux ( $H/LE$ ), also known as the Bowen ratio ( $\beta$ ) (Gavilán and Berengena, 2007). Using the energy balance equation and the Bowen ratio, H and LE can therefore be estimated as:

$$LE = \frac{R_n - G}{1 + \beta} \quad (3.4)$$

$$H = \frac{\beta}{1 + \beta} (R_n - G) \quad (3.5)$$

where H is the sensible heat flux and LE is the latent heat flux,  $R_n$  is the net radiation, and G is the soil heat flux, all in  $W\ m^{-2}$ . When incorporating the flux gradient equations for the two fluxes (LE and H), the Bowen ratio is given as:

$$\beta = \frac{H}{LE} = \frac{-\rho_a c_p K_H \left(\frac{\Delta T}{\Delta z}\right)}{-\frac{\rho_a c_p K_W}{\gamma} \left(\frac{\Delta e}{\Delta z}\right)} \quad (3.6)$$

This simplifies to:

$$\beta = \gamma \frac{K_H \Delta T}{K_W \Delta e} \quad (3.7)$$

where  $\gamma$  is the psychrometric constant ( $\text{J kg}^{-1} \text{ }^\circ\text{C}$ ),  $K_H$  and  $K_W$  are eddy diffusivities for sensible heat and water vapor respectively in  $\text{m}^2 \text{ s}^{-1}$ . These are also referred to as eddy exchange coefficients. These diffusivities are assumed to be equal, therefore allowing the Bowen ratio to be expressed as:

$$\beta = \gamma \frac{\Delta T}{\Delta e} \quad (3.8)$$

The  $\Delta T$  and  $\Delta e$  are air temperature ( $^\circ\text{C}$ ) and vapor pressure differences (kPa) between two levels at which these are measured, respectively.

The assumption of equal eddy exchange coefficients  $K_H$  and  $K_W$  is based on the fact that both heat and water vapor may be originating from the same source, and are carried by the same turbulent eddies, so they will remain correlated throughout the flow, resulting in their diffusivities being equal (McNaughton and Laubach, 1998).

The BREB technology is low cost, and therefore preferred in developing countries, and it is considered to be reliable (Lee et al., 2004). Todd et al. (2000) mention a few advantages of BREB; that it requires no information on the aerodynamic characteristics of the surface to calculate the fluxes, that it can estimate the fluxes at short time-steps, and that when connected to a data logger it can provide continuous data. One noted problem with BREB is that when  $\beta$  approaches -1, the denominators for both LE and H will tend to zero (see Equations 3.4 and 3.5), and that data would have to be excluded. According to Perez et al. (1999), that would normally be around sunrise and sunset. Therefore data where  $\beta$  is in the range  $-1.3 < \beta < -0.7$  are therefore usually excluded from the calculations of fluxes.

## **The BREB and advection**

As previously mentioned, one of the assumptions of the BREB method is that the ratio of the exchange coefficients for heat and water vapor is unity. However, it has been observed that these two coefficients are not equal under conditions of advection (Gavilan and Berengena, 2007; Lee et al., 2004; McNaughton and Laubach, 1998) and in such cases  $K_H$  may exceed  $K_W$ , which may lead to underestimation of ET. The objective of this chapter was to test the validity of the modified SEBAL model, especially to test its ability to account for advection for crops other than alfalfa, by comparing the model-estimated crop ET with the BREB-measured ET. It is, therefore, necessary that the observations are not affected by advection hence the need to discuss how advection affects the accuracy of the BREB method.

For the BREB approach to be accurate the measurement of air temperature and vapor pressure should be within the equilibrium sub-layer and the assumption is that there are no horizontal gradients. This can be ensured by adequate fetch (Todd et al., 2000), otherwise due to local advection, the mentioned assumption would not hold. Lee et al. (2004) pointed out that even with enough fetch, regional advection can affect the equality of diffusivities when the scalar (e.g., heat) is transported downward by large eddies from elevated inversion.

McNaughton and Laubach (1998) observed the  $K_H$  and  $K_W$  values over a well-watered wheat field, and noted that the median values for  $K_H/K_W$  were 0.79 when the gradient Bowen ratio was negative and 2.10 when it was positive and not 1 as assumed. However, they also mentioned that despite the observed inequality of  $K_H$  and  $K_W$  when BREB is used to estimate ET, only minor errors result, and BREB ET values remain comparable to other methods, like the eddy covariance system.

When Todd et al. (2000) compared the BREB with lysimeter for the estimation of latent heat flux, there was a variability of 5-15% during the day and higher at night, 25-45%, which did not result in significant error as the ET observations at night were less than 0.05 mm hr<sup>-1</sup>. Gavilán and Berengena (2007) observed that during the day, the accuracy of the BREB method under unstable atmospheric conditions differed from the accuracy under stable atmospheric conditions; with stable conditions resulting in the Bowen ratio method overestimating ET by 6.3% while with unstable conditions the overestimation was only 5.1%. They concluded that the error was minimal. Therefore, several researchers do agree that while the concerns about inequality of the turbulent exchange coefficients are valid, they do not result in significant systematic bias in the estimation of ET, only minimal errors are incurred.

## **Objectives**

This chapter sought to test the transferability of the modified SEBAL model. As the model was developed under standard conditions, this part of the research evaluated the model performance under non-standard surface conditions, which included different crops (beans, wheat, and corn) and different soil root zone water content (fully irrigated and with limited irrigation). The estimated ET was compared to ET measured using the Bowen Ratio Energy Balance method.

## **METHODS AND MATERIALS**

### **Study Area**

The area of study was the Limited Irrigation Research Farm (LIRF) near Greeley, CO, managed by the USDA-ARS water management research unit, Fort Collins, CO (Figure 3.1).

The farm is located at coordinates 40° 26' N and 104° 38' W, and the elevation of the area is 1,426 m above mean sea level (amsl). The area receives on average 360 mm of precipitation in a year. Data from two research fields were used in this study, one field referred to as the East field (E) and the other West (W). Both fields were under surface drip irrigation. In some years, one of the fields was treated to full irrigation while the other was under limited irrigation.

In each field a Bowen ratio-energy balance (BREB) system was installed, with the mast installed close to the center. Both systems were of the automatic exchange mechanism (AEM) type, with air temperature/relative humidity sensors on the arms switching positions every 15 minutes to avoid instrument bias (Todd et al., 2000). After switching, the sensors were allowed to equilibrate for 5 minutes, and then take measurements for 10 minutes before switching again. As the crops grew, the Bowen system was raised such that the lower arm was always a foot above the canopy, and the difference in level between the arms was kept at a meter.

The fields were also equipped with infrared thermometers (IRT, model S1-121, Apogee Instruments, Inc., Logan Utah, USA), in an oblique angle (about 45°) placed on poles on the north and south of the Bowen Ratio mast to measure the canopy temperature. These were initially at 2 m above the canopy until full canopy, then adjusted to be 1 m above the canopy, as long as the height of the stand allowed. Net radiometers, Q7 (REBS, CSI, Logan, Utah, U.S.A.) were installed to measure net radiation, and cup anemometers (G113, RM Young) for wind speed, both at 2 m above the canopy at all times. Soil heat flux plates (REBS model, HFT3, CSI, Logan, Utah, U.S.A.) were buried 8 cm below the ground surface, one in crop row and another between rows, and values were averaged. Thermocouples were buried 3-4 cm below soil surface to measure soil temperature, and soil water content was measured using Hydra Probe 11 sensors,

which were installed horizontally, with the middle prongs 4 cm below the surface. These too, were in pairs, one in crop row, and the other between rows and the values were averaged.

### **Satellite Data Requirements and image processing**

The modified SEBAL model was tested on a fully irrigated corn crop and also on corn under limited (deficit) irrigation for the cropping seasons 2010 and 2012. Landsat 5 Thematic Mapper (TM) and Landsat 7 Enhanced Thematic Mapper Plus (ETM+) satellite images were downloaded from the USGS Earth Explorer site. The model was tested for a wide ground cover range (10 – 94% for fully irrigated corn, and 2 – 78% for deficit irrigated corn). The corn height reached 280 cm for the fully irrigated corn and 220 cm for the deficit irrigated corn.

The model was tested on fully irrigated wheat during the 2009 and 2011 cropping seasons. It was also tested on beans grown in 2008 and also in 2010. During the 2008 cropping season, the test was performed with data from DOY 192, 200 and 224. During 2010, it was performed with data from DOY 198, 205 and 229. Table 3.1 shows the crops on which the model was tested.

The Landsat images were processed using the modified SEBAL model described in Chapter 2, and the final output was daily evapotranspiration ( $ET_{24}$ ) which was compared to actual ET measured using the Bowen Ratio Energy Balance (BREB) system. Performance indicators such as Mean Bias Error (MBE), Root Mean Square Error (RMSE) and the Nash-Sutcliffe Coefficient of Efficiency (NSCE) were used to evaluate how the estimated ET compared to the measured ET. These indicators are described in Chapter 1.

## RESULTS AND DISCUSSIONS

In Chapter 2, a semi-empirical method was used to model advection, or specifically effective advection. In doing so, a wind function as shown in Equation 3.9 was developed, with its parameters described in Chapter 2, Equation 2.19. The wind function included wind and temperature parameters. Instead of using the mean temperature as a surrogate for heat content of the transported air, maximum and minimum temperatures were used. The mean temperature masks the influence of the high temperatures on afternoon advection, so the maximum temperature was used instead, and the minimum temperature indicates how the air temperature in the evening may contribute to evening ET. Although minimum temperature may not take place until the early morning, it does give an indication of how temperature drops during the day, and hence give an idea of the possibility of evening ET.

$$f(u) = \frac{8\left(\frac{T_{max}}{20}\right)\left(\frac{T_{min}}{10}\right)\left(1+\frac{U}{100}\right)}{\left[\ln\left(\frac{z_2-d}{z_{om}}\right)\right]^2} \quad (3.9)$$

Results from using the modified SEBAL model were compared with BREB results for all corn (i.e. both fully irrigated and with limited irrigation, and the comparison is shown in Figure 3.2. The newly developed model seemed to do well in estimating ET, though there still seemed to be some minor errors in estimating ET for surfaces with low biomass such as in early stages of growth as shown in Figure 3.2 for lower ET values (lower values in x-axis). The statistics suggest a good performance of the model; the MBE was  $-0.6 \text{ mm d}^{-1}$  ( $-9.0 \%$ ), RMSE was  $1.45 \text{ mm d}^{-1}$  ( $21.2 \%$ ) and the NSCE was 0.36, which indicates that the model was appropriate in the estimation of ET.

Table 3.2 gives the ET values and corresponding instantaneous evaporative fraction as obtained from SEBAL processed images, and also the height of the corn is included in the table. In most cases there was underestimation of ET with lower EF. Table 3.2 shows the ET estimation using modified SEBAL on 18 June 2012, the field was fully irrigated, but the corn was still 0.31 m in height, and had  $EF_{inst}$  of 0.3, the ET error when compared to BREB was  $-3.2 \text{ mm d}^{-1}$  (-64.2 %) which was the largest underestimation observed. Other examples were on 30 June 2010 and 16 July 2010, when the  $EF_{inst}$  was 0.69 and 0.78 respectively and the ET errors were  $-3.0 \text{ mm d}^{-1}$  (-31.7 %) and  $-2.3 \text{ mm d}^{-1}$  (-25.6 %), respectively.

The errors observed for lower ET values were discussed in Chapter 1 and earlier in this chapter, and are associated with surface inhomogeneity as a result of sparse vegetation cover. The adjustment made on SEBAL is not meant to correct for such errors and therefore are still expected to occur. It is however worth pointing out that some work is being done by other researchers to increase the accuracy of remote sensing models when there is no full cover.

The error could also be due to the use of EF to determine the portion of advected energy that is used for evapotranspiration. In Equation 3.3, for well-irrigated areas, the EF is approximately 1. However, when there is lack of water in the soil, and the actual evapotranspiration becomes less than available energy, then EF becomes less than 1, and much less than 1 when the stress is severe. When using the original SEBAL, in the absence of advection, the energy used for evapotranspiration is obtained by multiplying EF with daily net radiation ( $Rn_{24}$ ).

In modified SEBAL, the advected energy component is assumed to use the same partitioning (i.e.  $EF \times E_{ad}$ ), as shown in Equation 3.3. This may not be accurate, as  $EF_{inst}$  has been estimated based on how solar radiation interacts with the surface, which can be considered

a vertical 'flow' of energy to the area, while advection is mostly horizontal. With advection being horizontal, there are added complexities, which include wind direction and crop row orientation. Thus, while in well-watered fields, the EF is insignificant as it is close to 1, in fields where the plants are water-stressed or where there is dry soil exposure, the assumption of the same EF for advection as the one used for net radiation may cause some error. It is important though to note that with drier surfaces, advection may have less effect such that correction may be unnecessary; however the challenge would be to identify the threshold of EF where advection becomes insignificant.

When the modified SEBAL model was used on only irrigated corn, where the EF was approximately 1, the results were as shown in Figure 3.3. Most of the points were along the 1:1 line, which means there was higher accuracy of the estimated ET when compared to BREB ET. The MBE was  $0 \text{ mm d}^{-1}$  which suggests no bias and RMSE was  $0.78 \text{ mm d}^{-1}$  (10.7 %) and the NSCE was 0.82. All ET errors were less than 15 % except on 18 July 2008 when the ET was overestimated by 1.6 mm (19.7 %). It was an advective day, with afternoon average wind speed being  $3.3 \text{ m s}^{-1}$  and the maximum temperature was  $30.7 \text{ }^{\circ}\text{C}$  and minimum temperature was  $14.5 \text{ }^{\circ}\text{C}$ , and the EF was 0.91.

One assumption may have caused an overestimation of ET on conditions of advection. The stomatal resistance is assumed to be embedded in the  $EF_{\text{inst}}$  that is determined using SEBAL at the time of satellite overpass, and the assumption is that the increase in evaporative demand due to the wind and warm air in the afternoon does not affect the stomatal resistance. However, that may not be the case as Zermeno-Gonzalez and Hipps (1997) observed an inverse relationship between canopy moisture conductance and saturation deficit at the canopy surface,

and different crops respond differently to the severity of advection. That may have caused the overestimation of ET in this case.

It must be noted that fully irrigated corn above a certain height, in this study, at around 0.9 m tend to have the same roughness length for momentum ( $z_{om}$ ), which in this case was 0.108 m. This is because SEBAL uses the vegetation index NDVI to determine  $z_{om}$ , which tends to saturate between 0.8-0.9. This agrees well with the fact that roughness increase with plant density up to a certain point whereby the surface is thereafter made smooth. Jacobs and van Bavel (1988) observed that the  $z_{om}$  for a corn crop tended to level off at a value of 0.12 m.

Figure 3.4 shows when the 24-hour wind speed had been used instead of the afternoon wind. There was slightly more error on ET estimation when the 24-hr wind was used than when the afternoon wind speed was used, with the MBE being -9.3 % compared to 0 % when afternoon wind speed was used.

The modified SEBAL model was then used on wheat and beans. Figure 3.5 shows the comparison of modified SEBAL ET and BREB ET for wheat and beans. The square symbols represent wheat while the diamond symbols represent beans. Most of the points were below the 1:1 line suggesting that the model underestimated ET for these crops. The MBE was  $-0.7 \text{ mm d}^{-1}$  (-11.3 %), and the RMSE was  $0.82 \text{ mm d}^{-1}$  (13.9 %) and the NSCE was 0.64. The RMSE was reasonably low, but the bias of -11.3 % would mean that the seasonal estimation of ET could be grossly underestimated. In most cases, the beans and wheat had a low EF (i.e. significantly lower than 1), which affects the accuracy as earlier alluded to. Also there were not enough images to conclude on the performance of the model on beans and wheat at various stages of growth.

## CONCLUSION

The modified SEBAL model was tested for transferability on crops and moisture conditions different from standard (alfalfa, 40-60 cm and not short of water). The crops used were corn, beans and wheat. Although the area where these were grown (near Greeley) had less severe advection than Rocky Ford, there were still some days when advection was significant. When the model was tested on wheat and beans, there was an underestimation indicated by an 11 % negative bias. This could have been because for most days when satellite images were available, the EF was significantly below 1 as the crops seemed not to cover the ground and the model does not perform ideally under those conditions.

The model was then tested on corn, and it was on fully irrigated corn, and also on corn treated to limited irrigation. For the fully irrigated corn, the model performed reasonably well. Since the advection-estimating sub-model had a roughness parameter embedded, it could sufficiently estimate advection and ET for a range of crop heights. When the model was used on corn with EF significantly less than 1, which includes corn at early stages of growth and fully-grown corn but water stressed, there were noticeable errors.

Concerning the early stages of growth, since the error is not due to advection, it was expected that the model would result in no significant improvement, as it was not the objective of the research to improve ET estimation under those conditions. However, even with corn at full cover, yet water-stressed, the model failed to adequately account for advection. This was thought to be due to the use of EF for the advection component of available energy. While EF may be accurate in defining the portion of  $Rn_{24}$  that is used for evapotranspiration, assuming the same fraction for advection may not be accurate, hence the errors observed.

## RECOMMENDATIONS

1. The modified SEBAL was found to be suitable for use on various crops which are well irrigated and therefore recommended for use in arid and semi-arid areas where SEBAL would underestimate because of its failure to account for advection, while there may not be enough weather data to be able to use METRIC.
2. Further research should be carried out to evaluate the appropriateness of applying the evaporative fraction (EF) on the advection component in the modified  $ET_{24}$  sub-model.
3. As some research is being done to improve the performance of remote sensing models when there is no full cover, such improvements should also be incorporated in this modified version of SEBAL

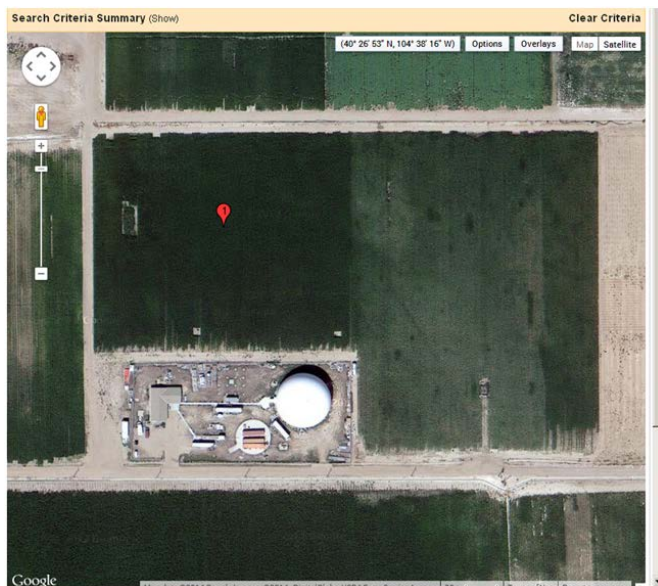


Figure 3.1: An aerial view of the two fields in LIRF

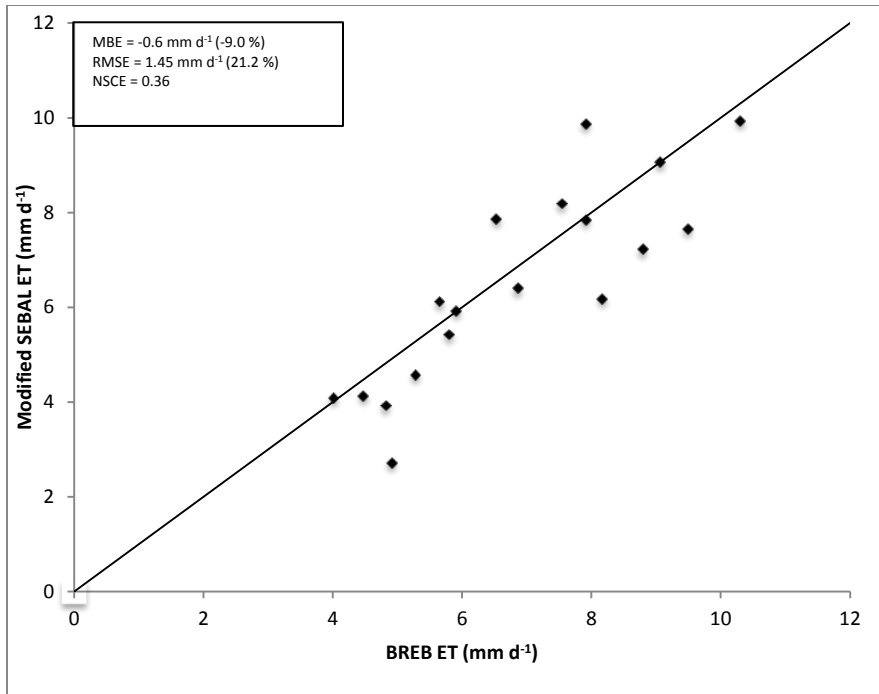


Figure 3.2: The modified SEBAL model ET compared to measured ET for corn (from limited and fully irrigated fields)

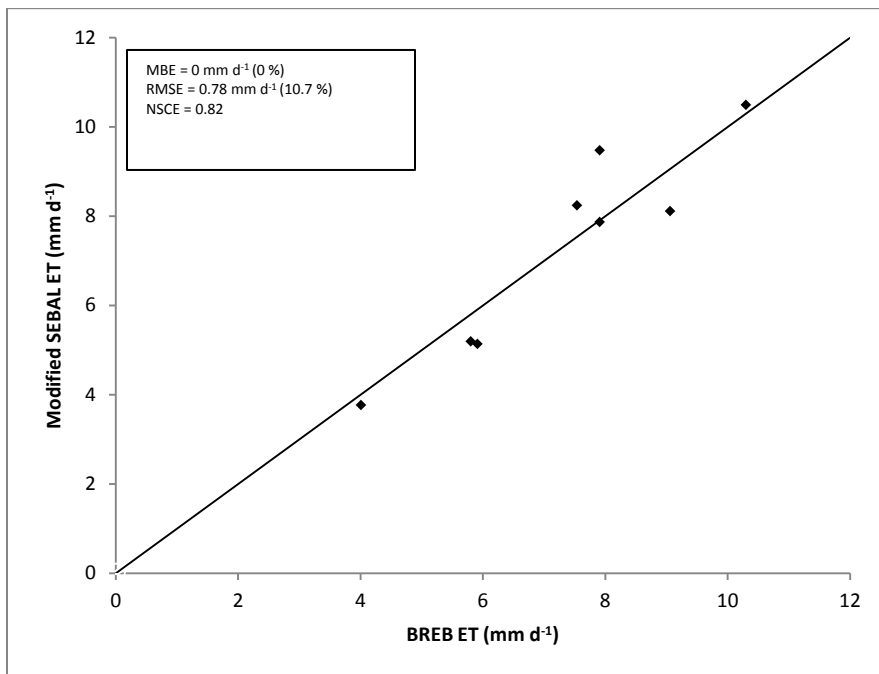


Figure 3.3: BREB ET compared to modified SEBAL ET for non-stress full cover corn

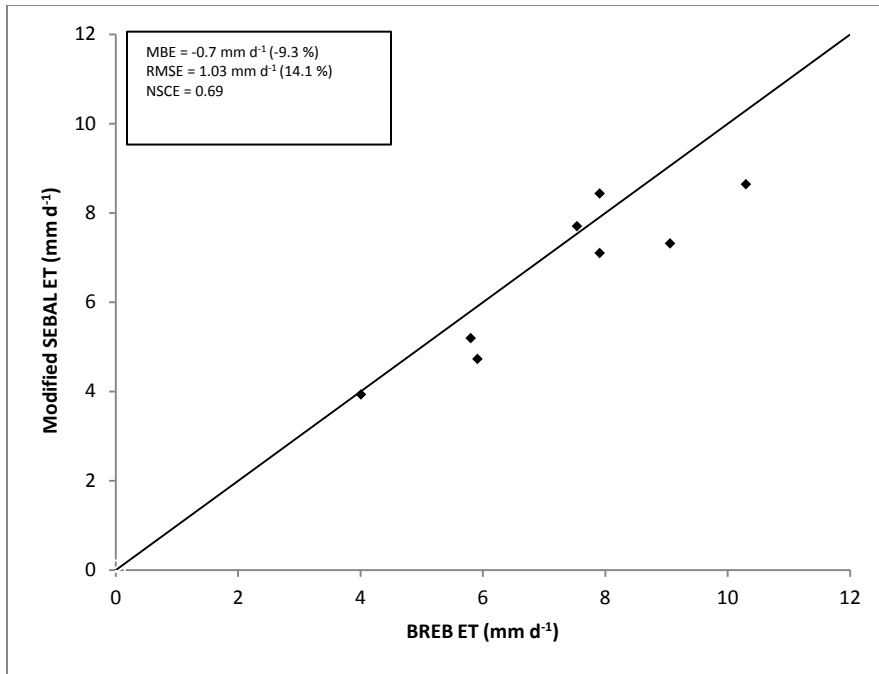


Figure 3.4: BREB ET compared to modified SEBAL ET for non-stress full cover corn when 24-hour wind speed was used.

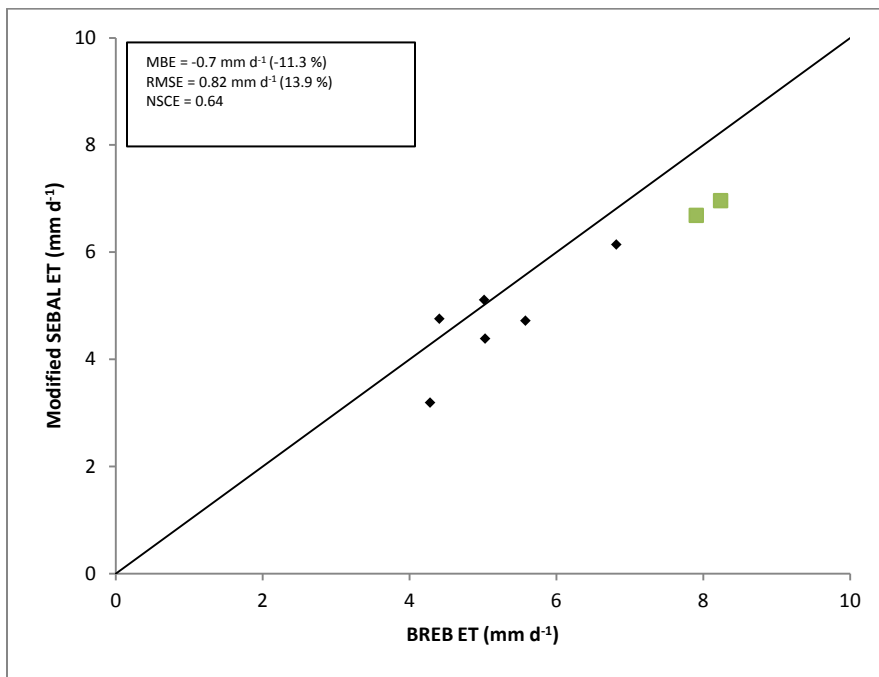


Figure 3.5: comparison of BREB ET and modified SEBAL ET for beans and wheat

Table 3.1: Crops grown at LIRF and used to test model.

<b>Year</b>	<b>Crop</b>	<b>Treatment</b>	<b>Field</b>
2008	Beans	Full irrigation	E
2009	Wheat	Full irrigation	W
2010	Beans	Full irrigation	E
2010	Corn	Full irrigation	W
2011	Wheat	Full irrigation	E
2012	Corn	Full irrigation	W
2012	Corn	Limited irrigation	E

Table 3.2: Comparison of Modified SEBAL-estimated ET and BREB ET for corn in LIRF, Greeley

<b>Date</b>	<b>Irrigation regime*</b>	<b>Crop height (m)</b>	<b>EF</b>	<b>BREB ET (mm)</b>	<b>Mod. SEBAL ET (mm)</b>	<b>% Error</b>
24-Jun-08	F	0.25	0.51	5.3	6.1	15
10-Jul-08	F	0.51	0.86	8.2	6.0	-26
11-Aug-08	F	2.29	0.96	5.9	5.8	-1
27-Aug-08	F	2.29	0.98	4.0	4.1	2
2-Jul-08	F	0.36	0.65	4.5	3.6	-19
18-Jul-08	F	1.02	0.91	7.9	10.7	35
30-Jun-10	F	0.80	0.69	9.5	6.5	-32
16-Jul-10	F	1.90	0.78	8.8	6.5	-26
17-Aug-10	F	2.60	0.96	5.8	5.4	-7
24-Jul-10	F	2.10	0.97	7.5	8.1	7
18-Jun-12	F	0.31	0.30	4.9	1.8	-64
18-Jun-12	L	0.47	0.44	4.8	2.9	-39
13-Jul-12	F	1.50	0.97	9.1	8.9	-1
13-Jul-12	L	1.51	0.94	7.9	7.7	-3
20-Jul-12	F	2.12	0.97	10.3	9.8	-5
20-Jul-12	L	1.88	0.87	6.5	7.5	14
5-Aug-12	F	2.60	0.95	6.9	6.3	-8
5-Aug-12	L	2.40	0.90	5.7	5.9	5

\* F = full irrigation, L = Limited irrigation

## REFERENCES

Allen RG, Tasumi M and Morse A (2005) Satellite-based evapotranspiration by energy balance for western states water management. US Bureau of Reclamation Evapotranspiration Workshop. February 8-10, 2005.

Arya SP (2001) Introduction to Micrometeorology. 2<sup>nd</sup> Ed. Academic Press. San Diego, USA.

Campbell GS and Norman JM (1998) An introduction to environmental biophysics. Second edition. Springer. NY, USA.

Gavilán P and Berengena J (2007) Accuracy of the Bowen ratio-energy balance method for measuring latent heat flux in a semi-arid advective environment. *Irrig. Sci.* 25: 127-140.

Gay LW and Bernhofer C (1991) Enhancement of evaporation by advection in arid regions: Hydrological interactions between atmosphere, soil and vegetation. Proceedings of the Vienna Symposium, August 1991. IAHS Publ. no. 204.

Gieske A and Meijninger W (2005) High density NOAA time series of ET in the Gediz Basin, Turkey. *Irrigation and Drainage Systems* 19:285-299.

Hatfield JL (1989) Aerodynamic properties of partial canopies. *Agricultural and Forest Meteorology* 46:15-22.

Jacobs AFG and van Bavel JH (1988) Changes of the displacement height and roughness length of maize during a growing season. *Agricultural and Forest Meteorology* 42:53-62.

Lee X, Yu Q, Sun X, Liu J, Min Q, Liu Y, Zhang X (2004) Micrometeorological fluxes under the influence of regional and local advection: a revisit. *Agricultural and Forest Meteorology* 122:111-124.

Mašková Z, Zemek F, Květ J (2008) Normalized difference vegetation index (NDVI) in the management of mountain meadows. *Boreal Environment Research* 13:417-432.

Matthias AD, Kustas WP, Gay LW, Cooper DI, Alves LM, Pinter (Jr.) PJ (1990) Aerodynamic parameters for a sparsely roughened surface composed of small cotton plants and ridged soil. *Remote Sens. Environ.* 32:143-153.

McNaughton KG and Laubach J (1998) Unsteadiness as a cause of non-equality of eddy diffusivities for heat and vapour at the base of an advective inversion. *Boundary-Layer Meteorology* 88:479-504.

Morse A, Tasumi M, Allen RG, Kramber WJ (2000) Application of SEBAL Methodology for estimating consumptive use of water and streamflow Depletion in the Bear River Basin of Idaho through remote sensing. Final Report submitted to Raytheon Systems Company.

Paul G, Gowda PH, Prasad PVP, Howell TA, Staggenborg SA, Neale MUN (2013) Lysimetric evaluation of SEBAL using high resolution airborne imagery from BEAREX08. *Advances in Water Resources*, 59: 157-168.

Perez PJ, Castellvi F, Ibañez M, Rosell JI (1999) Assessment of reliability of Bowen ratio method for partitioning fluxes. *Agricultural and Forest Meteorology* 97:141-150.

Prueger JH, Kustas WP, Hipps LE, Hatfield JL (2004) Aerodynamic parameters parameters and sensible heat flux estimates for a semi-arid ecosystem. *Journal of Arid Environments* 57:87-100.

Raupach MR (1994) Simplified expressions for vegetation roughness length and zero-plane displacement as functions of canopy height and area index. CSIRO Centre for Environmental Mechanics. Research note.

Singh RK, Irmak A, Irmak S, Martin DL (2008) Application of SEBAL Model for mapping evapotranspiration and estimating surface energy fluxes in South-Central Nebraska. *Journal of Irrigation and Drainage Engineering*, 134 (3): 273-285

Shuttleworth WJ and Wallace JS (1985) Evaporation from sparse crops – an energy combination theory. *Quart. J. R. Met. Soc.* 111: 839-855.

Todd RW, Evett SR, Howell TA (2000) The Bowen ratio energy balance method for estimating latent heat flux of irrigated alfalfa evaluated in a semi-arid, advective environment. *Agric. For. Meteorol.* 103:335-348.

Zermeño-Gonzalez A and Hipps LE (1997). Downwind evolution of surface fluxes over a vegetated surface during local advection of heat and saturation deficit. *Journal of Hydrology* 192: 189-210.

## CHAPTER 4

### CONCLUSION

#### Overview

In recent years several remote sensing (RS) models have been developed to estimate evapotranspiration (ET). The use of remote sensing brings some unique advantages in the management of water used for agricultural purposes. Some of these advantages are that it enables ET mapping of a large area, which makes the management of water at large scale feasible. The use of RS algorithms also provides a tool to estimate actual crop water use, and can be compared with deliveries to determine irrigation efficiencies. There are several methods that can be used to directly or indirectly measure ET, but the instrumentation is complex and/or expensive, not portable, and most of them represent point measurements, at best measuring as much as a field.

As water scarcity seems to be increasing, more water management techniques have to be employed, including RS methods. Recently, scientists have introduced several RS algorithms in the research of water management and some are now implemented in the field. However, few of these are suitable for use in areas where data, especially weather data, might be limited such as in developing countries. The Surface Energy Balance Algorithm for Land (SEBAL) model requires minimal weather data; only wind speed at the time of satellite overpass, and in some cases may require solar radiation that has accumulated in a day. Most developing countries would normally only have daily wind run, minimum and maximum air temperatures, wet bulb temperature and sunshine hours. SEBAL would also not require prior knowledge of surface conditions. However, knowledge of the area where the ET is estimated would be an advantage in some cases.

The fact that this model requires less data is one the reasons that has enabled SEBAL to be widely used, i.e. in several countries of varying geographical and climatic conditions. However, it has been observed that SEBAL does not always perform well in semi-arid and arid areas due to the model's inability to account for advection. This results in the underestimation of ET in such areas. To resolve this challenge, an improvement to SEBAL was developed - Mapping Evapotranspiration with Internalized Calibration (METRIC) model that better responded to effects of advection. However, METRIC requires good quality weather data at hourly time steps; which makes it unsuitable for most developing countries. This research therefore sought to improve SEBAL, to better account for advection, but with limited weather data; data that is likely to be available in most developing countries. The required weather data is minimum and maximum air temperature; wind run, wet bulb temperature, and measurements of solar radiation if available.

The approach employed in this research was to model the advection responsible for ET enhancement, which is termed “effective advection”, and include it in the 24-hour ET sub-model of SEBAL ( $ET_{24}$ ):

$$ET_{24} = \frac{86,400 \times EF \times (Rn_{24} + \lambda E_{ad})}{\lambda \times \rho_w} \quad (4.1)$$

The conclusions drawn from this study were:

**On the performance of SEBAL and METRIC:**

- SEBAL tends to underestimate ET when there is advection, and this is because it has no function that responds to the presence of advection, and only regards radiation from the sun as the only source of energy for evapotranspiration over the day.
- METRIC on the other hand matched measured ET better than SEBAL on days when there was advection.
- Both models had problems estimating ET at early growth stages when canopy ground cover was low. This was attributed to the fact that at early stages of crop growth, the surface is heterogeneous, i.e. there is part canopy and part exposed soil. These two models are referred to as single-source RS models, and that means the whole surface is represented as a single layer in these models.
- From observations, it was indicated that wind is related to advection; other variables (i.e., air temperature and vapor pressure) were also related. There was a strong correlation especially between afternoon wind speed and advection.

### **Modification of SEBAL to account for advection:**

- It is possible to model effective advection and incorporate it in the SEBAL model, and this may result in a more accurate estimation of ET. Comparing the alfalfa ET obtained using modified SEBAL and original SEBAL (using lysimeter measurements as standard), the modified SEBAL resulted in Mean Bias Error of  $0.17 \text{ mm d}^{-1}$  (2.2 %) while the original SEBAL had MBE of  $-1.3 \text{ mm d}^{-1}$  (-17.1 %), which showed a significant improvement.
- It was also noted that the quality of modified SEBAL to significantly reduce bias makes it important for the accurate estimation of seasonal ET.

### **Transferability of model to various surface conditions:**

- When the modified SEBAL model was tested on other crops i.e. wheat, beans and corn, there was observed some underestimation in wheat and bean, most likely because there were only a few images where the crop completely covered the ground, in most there was heterogeneity, which as earlier observed, the model does not perform well under those conditions.
- On fully-irrigated corn, the model performed reasonably well, with less error, though on one instance, on a very advective day, the model seemed to overestimate ET, possibly because it does not mimic the increase in stomatal resistance that may result from increase in evaporative demand on very advective afternoons.

- When the model was used on water-stressed corn or corn at earlier stages of growth, errors indicated that it was less suitable for such conditions. However, under such conditions, the effective advection would most likely be small, since advection would enhance sensible heat flux rather than latent heat flux (ET).

### Summary of modification

The following are the steps in the correction for advection:

1. Wind function:

$$f(u) = \frac{8\left(\frac{T_{max}}{20}\right)\left(\frac{T_{min}}{10}\right)\left(1 + \frac{U}{100}\right)}{\left[\ln\left(\frac{Z_2-d}{z_{om}}\right)\right]^2} \quad (4.2)$$

where U is the afternoon wind speed average in  $\text{m s}^{-1}$  and temperatures are in Celsius.

2. Drying power of the atmosphere:

$$E_a = f(u) \times (e_s - e_a) \quad (4.3)$$

where  $e_s$  and  $e_a$  are saturated vapor pressure and actual vapor pressure calculated as outlined in the ASCE-EWRI Standardized Penman Monteith ET procedure (ASCE-EWRI, 2005), and these are in kPa.

3. ET enhancement, which is the water depth equivalent of effective advection:

$$ET_{ad24} = \frac{\gamma}{\Delta + \gamma} E_a \quad (4.4)$$

4. The adjusted  $ET_{24}$  model is given as:

$$ET_{24} = \frac{86,400 \times EF \times (Rn_{24} + \lambda E_{ad})}{\lambda \times \rho_w} \quad (4.5)$$

### **Model Limitation (s)**

The model developed was found to be effective in accounting for advection and because it has an aerodynamic component, it could be used for various types of crops. Similar to the original SEBAL, and even METRIC, this modified SEBAL is inaccurate in the estimation of ET at low biomass or in water-stressed fields, which include the early stages of crop growth. More investigation can be done to see how the model can be further modified so that it accurately estimates under any situation. However, if the current modified model were to be used in areas under adequate irrigation, it would suffice.

## APPENDICES

Table A1: Comparison of modeled alfalfa hourly ET and lysimeter-measured alfalfa hourly ET

<b>Date</b>	<b>Lysimeter ET (mm h<sup>-1</sup>)</b>	<b>SEBAL ET (mm h<sup>-1</sup>)</b>	<b>METRIC ET (mm h<sup>-1</sup>)</b>	<b>NDVI</b>
15 June 10 (A)	0.64	0.76 (19)	0.61 (5)	0.64
01 July 10(A)	1.04	0.84 (-20)	0.90 (14)	0.81
02 Aug 10(A)	0.77	0.86 (11)	0.75 (3)	0.81
18 Aug 10(A)	0.85	0.84 (-1)	0.81 (5)	0.84
19 Sep 10(A)	0.56	0.71 (26)	0.58 (-3)	0.82
05 Oct 10(A)	0.68	0.63 (-7)	0.59 (13)	0.81
18 June 11(A)	0.72	0.58 (-19)	0.72 (0)	0.59
04 July 11(A)	0.97	0.87 (-11)	0.91 (7)	0.83
05 Aug 11(A)	0.74	0.87 (17)	0.73 (2)	0.84
21 Aug 11(A)	0.91	0.82 (10)	0.78 (14)	0.83
04 June 12(A)	0.96	0.64 (34)	0.77 (20)	0.51
20 June 12(A)	1.06	0.88 (-17)	0.85 (19)	0.80
22 July 12(A)	1.10	0.82 (-25)	0.81 (26)	0.79
15 June 10(B)	0.57	0.75 (32)	0.68 (-16)	0.71
18 Aug 10(B)	0.14	0.11 (-21)	0.10 (27)	0.14*
19 Sep 10(B)	0.15	0.03 (-118)	0.06 (142)	0.13*
05 Oct 10(B)	0.41	0.07 (-83)	0.05 (89)	0.22*
18 June 11(B)	0.73	0.47 (-35)	0.57 (21)	0.48
05 Aug 11(B)	0.74	0.85 (15)	0.70 (5)	0.80
21 Aug 11(B)	0.82	0.80 (-2)	0.75 (8)	0.82
04 June 12(B)	0.79	0.48 (-39)	0.60 (24)	0.41

Table A2: Comparison of modeled alfalfa daily ET and lysimeter-measured alfalfa daily ET

<b>Date</b>	<b>Lysimeter ET (mm d<sup>-1</sup>)</b>	<b>SEBAL ET (mm d<sup>-1</sup>)</b>	<b>METRIC ET (mm d<sup>-1</sup>)</b>	<b>NDVI</b>
15 June 10 (A)	7.8	7.2 (-8)	6.6 (16)	0.64
01 July 10(A)	13.1	7.4 (-44)	11.0 (16)	0.81
02 Aug 10(A)	7.8	7.2(-8)	6.9 (12)	0.81
18 Aug 10(A)	7.7	6.5 (-16)	7.3 (5)	0.84
19 Sep 10(A)	7.7	4.6 (-41)	6.7 (13)	0.82
05 Oct 10(A)	6.6	3.6 (-46)	5.2 (22)	0.81
18 June 11(A)	8.1	5.8 (-29)	7.3 (9)	0.59
04 July 11(A)	11.2	7.5 (-33)	9.6 (14)	0.83
05 Aug 11(A)	7.9	7.5 (-6)	7.0 (12)	0.84
21 Aug 11(A)	8.4	6.3 (-25)	7.2 (14)	0.83
04 June 12(A)	9.4	5.8 (-38)	7.5 (20)	0.51
20 June 12(A)	13.3	7.7 (-42)	10.0 (25)	0.80
22 July 12(A)	14.2	7.3 (-48)	9.6 (33)	0.79
15 June 10(B)	8.1	7.8 (-5)	7.7 (9)	0.71
18 Aug 10(B)	1.4	1.2 (-18)	0.9 (36)	0.14*
19 Sep 10(B)	2.3	0.0 (-100)	0.7 (68)	0.13*
05 Oct 10(B)	4.3	0.5 (-88)	0.4 (91)	0.22*
18 June 11(B)	8.4	4.7 (-44)	5.8 (31)	0.48
05 Aug 11(B)	7.9	7.4 (-6)	6.7 (15)	0.80
21 Aug 11(B)	7.6	6.1 (-20)	6.9 (10)	0.82
04 June 12(B)	7.3	4.7 (-35)	5.9 (19)	0.41

\*the field was bare

A – Field A

B – Field B

Values in parenthesis are errors in percentage  $(O - M)/M \times 100$

Table A3: Comparison between calculated and measured net radiation on cloudy and cloudless days

Date	<sup>1</sup> Calc. $R_a$ ( $W m^{-2}$ )	<sup>2</sup> Calc. $R_n$ ( $W m^{-2}$ )	<sup>3</sup> Meas. $R_n$ ( $W m^{-2}$ )	<sup>4</sup> Error ( $W m^{-2}$ )	<sup>5</sup> Cloud cover
5/3/10	443.3	171.2	157.3	13.9 (9 %)	Y
5/4/10	445.0	171.9	157.3	14.6 (14.6 %)	Y
5/5/10	446.6	172.8	157.0	15.5 (10 %)	Y
7/28/10	457.9	192.0	186.9	5.1 (5.1 %)	Y
7/29/10	456.5	190.8	190.2	0.6 (0 %)	Y
8/13/10	432.0	171.9	171.5	0.4 (0 %)	Y
8/14/10	430.1	171.1	174.2	-3.1 (-2 %)	Y
9/14/10	357.6	125.9	132.4	-6.5 (-5 %)	Y
9/16/10	352.2	121.2	131.6	-10.4 (-8 %)	Y
9/18/10	346.8	116.7	126.6	-9.9 (-8 %)	Y
10/3/10	305.0	93.9.0	110.6	-16.7 (-15 %)	Y
5/1/10	439.8	171.6	144.5	27.1 (19 %)	N
5/2/10	441.6	170.9	122.2	48.7 (40 %)	N
5/17/10	463.7	183.3	171.7	11.6 (7 %)	N
7/30/10	455.1	189.6	154.5	35.1 (23 %)	N
8/15/10	428.2	164.2	98.4	65.8 (67 %)	N
9/30/10	313.4	98.0	105.7	-7.7 (-7 %)	N
10/1/10	310.6	96.2	106.1	-9.9 (-9 %)	N
10/2/10	307.8	92.6	70.2	22.7 (22 %)	N

<sup>1</sup>calculated extraterrestrial radiation

<sup>2</sup>calculated net radiation based on SEBAL-determined albedo

<sup>3</sup>net radiation measured using net radiometer in Field A

<sup>4</sup>discrepancy between measured and calculated net radiation, with % discrepancy in parenthesis

<sup>5</sup>indicator of whether it was a cloudless or cloudy day, Y=cloudless, N=cloudy

## Appendix A4: Steps in development of the advection model

1. Standard days (alfalfa of height between 40 and 60 cm, and not short of water) were used in the development of the advection model.
2. The model was based on the equation:

$$\lambda ET_{24} = R_{n24} + \lambda E_{ad24}$$

where  $\lambda ET_{24}$  was obtained by converting the lysimeter-measured ET in units of mm to energy equivalent,  $R_{n24}$ , which is the daily available energy, was measured in the field using a net radiometer.

3. By back-calculation, the advective component,  $\lambda E_{ad24}$ , was determined, and equated to:

$$\lambda ET_{ad24} = \frac{\gamma}{\Delta + \gamma} E_a$$

where  $\gamma$  and  $\Delta$  could be determined by temperature readings at the site., and  $E_a$  is the drying power of the air, and is given as the product of vapor pressure difference and the wind function:

$$E_a = f(u) \times (e_s - e_a)$$

4. On first trial, Stigter (1980)'s wind function was used as shown below:

$$f(u) = \frac{8(1 + \frac{U}{100})}{[\ln \frac{(z_2 - d)}{z_{om}}]^2}$$

4. Modifications were then made to the Stigter's model; the optimization objective was to have the Mean Bias Error (MBE) as close to zero as possible, while achieving a low root mean square error (RMSE).

$$f(u) = \frac{8\left(\frac{T_{max}}{20}\right)\left(\frac{T_{min}}{10}\right)\left(1 + \frac{U}{100}\right)}{\left[\ln\left(\frac{z_2 - d}{z_{om}}\right)\right]^2}$$